NASA TECHNICAL MEMORANDUM

NASA TM X-2553

NASA TM X-2553

PRELIMINARY EXPERIMENTS ON THE NOISE GENERATED BY TARGET-TYPE THRUST REVERSER MODELS

by Orlando A. Gutierrez and James R. Stone

Lewis Research Center
Cleveland, Ohio 44135

NATIONAL AERONAUTICS AND SPACE ADMINISTRATION • WASHINGTON, D. C. • MAY 1972

1. Report No.	2. Government Accession No.	3. Recipient's Catalog No.
NASA TM X-2553		

4. Title and Subtitle	5. Report Date
PRELIMINARY EXPERIMENTS ON THE NOISE GENERATED BY TARGET-TYPE THRUST REVERSER MODELS	May 1972
	6. Performing Organization Code
7. Author(s)	8. Performing Organization Report No.
Orlando A. Gutierrez and James R. Stone	E-6707
9. Performing Organization Name and Address	10. Work Unit No.
Lewis Research Center National Aeronautics and Space Administration Cleveland, Ohio 44135	764-72
	11. Contract or Grant No.
	13. Type of Report and Period Covered
12. Sponsoring Agency Name and Address	Technical Memorandum
National Aeronautics and Space Administration Washington, D.C. 20546	14. Sponsoring Agency Code

15. Supplementary Notes

16. Abstract

Experiments are reported on the noise generated by model V-gutter and semicylindrical target-type reversers with circular nozzles. Nozzles were 5.24 and 7.78 cm in diameter. Nozzle pressure ratio ranged from 1.25 to 1.72. The spacing between reversers and nozzle, as well as the reverser orientation, was also varied. Considerably more noise was generated with reversers than with the nozzle alone. The measured maximum overall sound pressure level varied with the sixth power of the nozzle exit velocity. Noise levels were much more uniform in regard to directivity with reversers than with the nozzle alone. Thrust reversers, therefore, can be a significant noise problem, especially for STOL aircraft using thrust reversers during approach.

17. Key Words (Suggested by Author(s))

Thrust reversers
Noise level
STOL aircraft
Acoustic
Experimental

18. Distribution Statement

Unclassified - unlimited

19. Security Classif. (of this report)	20. Security Classif. (of this page)	21. No. of Pages	22. Price*
Unclassified	Unclassified	61	$3.00

*For sale by the Clearinghouse for Federal Scientific and Technical Information
Springfield, Virginia 22151

PRELIMINARY EXPERIMENTS ON THE NOISE GENERATED BY TARGET-TYPE THRUST REVERSER MODELS

by Orlando A. Gutierrez and James R. Stone

Lewis Research Center

SUMMARY

A series of experiments is reported herein on the noise generated by target-type thrust reversers. "V"-gutter and semicylindrical thrust reversers were tested with a 5.24-centimeter-exit-diameter nozzle; a 7.78-centimeter nozzle was also tested with a cylindrical reverser. The ratio of reverser frontal area to nozzle area ranged from 2.45 to 7.01. The spacing between reverser and nozzle was varied from 0 to 1.61 nozzle diameters. The reverser orientation was also varied. Nozzle pressure ratio ranged from 1.25 to 1.72.

Considerably more noise was generated when the thrust reversers were used than with the nozzle alone, indicating that thrust reversal can be a significant noise problem for jet short-takeoff-and-landing (STOL) aircraft. In addition, reverser noise levels were much more uniform in regard to directivity than those of the nozzle alone. This would increase the time of exposure to sideline noise in excess of a particular level for a jet STOL aircraft landing with thrust reversers.

The measured maximum overall sound pressure level varied with the sixth power of the nozzle exit velocity.

INTRODUCTION

Since the ability to land in short distances is a requirement for STOL aircraft, jet thrust reversers may be necessary both for reducing the ground roll after landing and for steepening the approach flightpath. In STOL configurations such as the augmentor wing concept described in references 1 and 2, high engine speeds would be required during approach, thus almost necessitating at least partial thrust reversal. At the same time, because of the required capability to operate from airports in heavily populated areas, STOL aircraft will have to meet much more severe noise limitations than conventional aircraft.

There have been many studies on the aerodynamic performance of small-size thrust reversers of diverse types, such as those reported in references 3 to 7. Reports are also numerous on the behavior of full-scale reversers as described in references 8 to 11. Design reports, such as references 12 to 14, are also available in the literature. In addition, reports on applications of thrust reversers to commercial aircraft are available (refs. 15 to 17).

As indicated by the many references and applications cited, the aerodynamic behavior of thrust reversers has been extensively studied and documented. However, this has not been the case with regard to the noise generated by thrust reversers. For future STOL aircraft, noise will need to be considered. Thus, the present study was undertaken at the Lewis Research Center, and noise data on thrust reversers are presented herein.

The objective of this study was to determine the gross effects of reverser shape, size, spacing, orientation, and flow rate on the noise produced by target-type reversers. Target-type reversers were chosen for this study, primarily because of their simplicity. They can be built in many variations, as shown in figure 1. The noise data reported herein were obtained by using the "V"-gutter with cover plates (fig. 1(d)) and the semicylinder configurations (fig. 1(f)). The noise data reported cover a range of flow rates, reverser-frontal-area-to-nozzle-area ratios and spacing-to-nozzle-diameter ratios.

APPARATUS

Two separate flow systems were used to obtain the experimental data. The main system was an acoustic apparatus, designed to minimize internal noise and instrumented to obtain detailed acoustic data. A flow apparatus was used to obtain aerodynamic data and qualitative noise data prior to running the acoustic program. This preliminary screening of operating conditions was useful in setting up a proper test program with minimum operating time on the acoustic apparatus. The test configurations were obtained by various combinations of two different-sized nozzles with three small-scale reversers. The position of the reversers relative to the nozzles was varied through use of an adjustable mounting stand.

Acoustic Apparatus

The acoustic apparatus is shown in figure 2. Compressed air from a 1000-kN/m^2 abs source was supplied to the test nozzles at ambient temperature by a 10-centimeter-

nominal-diameter pipe. This pipe was equipped with an orifice for flow measurement, a 10-centimeter-diameter flow control valve, acoustic mufflers, and a straight section ending at the nozzle. The test reversers were mounted on an independent stand near the nozzle exit. The airflow system was set on a horizontal plane 122 centimeters above ground level. Details of this facility are given in reference 18.

The noise data were measured by eight condenser microphones with individual wind screens. The microphones were located on a 3.05-meter-radius semicircle centered on the nozzle outlet. The microphone circle was at the same elevation from the smooth asphalt ground surface as the nozzle centerline (122 cm). The microphone angular locations θ were measured from the upstream nozzle axial centerline. The microphones were located at 10°, 30°, 50°, 65°, 80°, 100°, 130°, and 160° for most of the configurations tested. (Symbols are defined in the appendix.)

Figure 3 is a detail of the air supply system near the nozzle, showing the mounting flange located approximately 50 centimeters upstream of the nozzle. This detail also shows dimensions of the two test nozzles used.

Flow Apparatus

The flow apparatus is shown in figure 4 and described in detail in reference 19. It was located in a relatively small chamber, and any noise measurements taken in this facility had value only as relative comparisons between one run and another. A portable sound level meter was placed 86 centimeters from the nozzle exit at a 90° angle to its axis to obtain the relative noise data. No thrust measurements were made.

Thrust Reversers

The small-scale reversers used in this experimental program are illustrated in figures 5 and 6. As indicated before, two different types of target reversers were studied: semicylindrical and V-gutter with cover plates.

Semicylindrical reversers. - Two semicylindrical thrust reversers were used, the only difference between them being the distance between side plates. The conversion from one to the other was made with removable inserts next to the side plates. The smaller semicylindrical reverser is shown in figure 5(a). The inserts along the side plates are very noticeable. The larger semicylindrical reverser is shown in figure 5(b). The significant dimensions for both reversers appear in figure 5(c). A nut welded to the rear of the cylindrical wall allowed mounting of the reversers to a threaded rod.

V-gutter-with-cover-plates reverser. - Only one variation of this reverser, herein called the V-gutter, was studied. Figure 6(a) shows the V-gutter, with the side plates mounted at 90° to each other and the cover plates. The reverser was connected to a threaded rod by means of a threaded plate at the rear of the reverser. Figure 6(a) shows the cover plates overlapping the side plates. This overlap was 1.9 centimeters. Figure 6(b) is a sketch of the V-gutter, giving pertinent dimensions.

Nozzle-Reverser Combinations

The three small-scale reversers were each mounted behind one of the two interchangeable nozzles by an adjustable mount which allowed easy substitution of reversers and quick adjustment of the spacing between nozzle and reverser, as well as change in the angular position of the reverser. Figure 7 shows both the V-gutter and larger semicylindrical reversers mounted in the horizontal ($\alpha = 0^{\circ}$) and vertical ($\alpha = 90^{\circ}$) attitudes. The smaller semicylindrical reverser was tested with both the 5.24- and the 7.78-centimeter-diameter nozzles, giving reverser frontal-area-to-nozzle-area ratios A_f/A_n of 5.63 and 2.55. The larger semicylindrical and V-gutter reversers were tested only with the 5.24-centimeter-diameter nozzle, giving area ratios A_f/A_n of 7.02 and 2.43, respectively. The area ratios and other dimensionless relations of the nozzle-reverser combinations appear in table I.

PROCEDURE

Program

The shapes of the reversers were chosen for simplicity. Their size, as indicated by their frontal-area-to-nozzle-area ratio A_f/A_n was selected to fall within the zone of maximum reverse-thrust ratio as determined by Povolny, Steffen, and McArdle (refs. 3 and 7).

The effect of the reverser-to-nozzle spacing on the aerodynamic performance of target-type reversers was also determined in reference 3. For any given configuration the maximum efficiency was obtained at the closest possible spacing that did not decrease the mass flow through the nozzle. Decreasing the spacing from this value sharply decreased the reverser efficiency. Increasing the spacing decreased the efficiency only very slightly if at all.

The range of spacings needed for noise testing of the present small-scale reversers was determined experimentally. A series of tests were run on the flow apparatus to determine the effect of spacing on flow rate at constant values of nozzle inlet pressure.

The results of these tests are given in table II. In addition to the flow, pressure, and spacing data, noise indications from the 20-kilohertz scale of a portable sound meter were also recorded. The spacing of the reversers from the nozzle x was selected as the distance from the nozzle exit to the free edge of the reverser side plates for all cases. Spacing ratio was defined as the ratio of this distance to the diameter x/D_n. Based on the results of these tests, the program for the acoustic tests was established. In addition to the spacing effects, the effects of velocity and orientation were studied on the acoustic apparatus.

The effect of velocity was studied by varying the nozzle pressure ratio through the manually operated 10-centimeter-diameter throttle valve. Nozzle pressure ratio P_n/P_a was defined as the ratio of nozzle inlet total pressure to atmospheric pressure.

The effect of orientation was studied by rotating the reversers 90°. With the reversers on the horizontal plane ($\alpha = 0^\circ$), the reversed air jets were on the same plane with the nozzle, pipe system, and microphones. With the reversers vertical ($\alpha = 90^\circ$), the reversed jets were in a plane at 90° to the microphone plane.

The conditions for each of the tests run on the acoustic facility are listed in table III, along with some of the major results. In addition to the 21 reverser tests, two runs (1 and 19) were made with the 5.24-centimeter-diameter nozzle with no reverser.

Experimental Procedure

Except for the angular locations of the eight microphones, which were varied slightly from one running date to the other (as shown in the appropriate tables and figures), the experimental procedure was the same for all acoustic tests. The nozzle-reverser combination was set for the proper spacing and orientation. Flow of unheated compressed air was established and regulated by the hand-operated throttle valve. The controlled parameter was the nozzle inlet pressure P_n. After flow conditions were stabilized, flow parameters and atmospheric conditions were recorded and three noise data samples were recorded for each microphone location. Noise data were analyzed directly by a 1/3-octave-band spectrum analyzer. The analyzer determined, for each microphone and sample, the sound pressure level (SPL) on each 1/3-octave band from 50 to 20 000 hertz. This information was placed on tape for computer processing.

The microphones were calibrated at the start of each day's operation with a standard piston calibrator. The data acquisition and analysis system was further checked as indicated in detail in reference 18.

Noise Data Analysis

Details of the analysis procedure used in processing the noise data are presented in reference 18. Mainly, the procedure makes corrections to the spectral data from the analyzer for the microphone-cable system, when necessary, and for atmospheric losses. The corrected SPL from all three samples are then compared (ref. 18) for reliability purposes and averaged arithmetically if found compatible. The averaged values of SPL are then analyzed to obtain the OASPL for each microphone. The spectral sound power level (PWL) and the total sound power level (OAPWL) were calculated by using the SPL values. The PWL for each 1/3-octave band is obtained by integrating over a hemisphere with a radius equal to the microphone circle radius. This assumes that all radiated sound impinging on the ground is reflected into the hemisphere. This also implies that all the SPL's reported are 3 decibels above free-field values. In addition, the spectral values have not been corrected for discrete reinforcements and cancellations. With the microphones set on a 3.05-meter-radius circle and 122 centimeters above ground, cancellations should occur in the 200-, 630-, and 1000-hertz 1/3-octave bands. Reinforcements should appear on the 400- and 800-hertz 1/3-octave bands.

RESULTS AND DISCUSSION

The data obtained are tabulated in tables II to IV. These data are also presented in graphical form in figures 8 to 23. No wind speed data are recorded as it never exceeded 2 meters per second.

Reversed flow patterns obtained during the tests were observed; for all reversers, the flow exited along the side plates. Only an insignificant amount of flow left the V-gutter reverser along the cover plates or the cylindrical reversers along the edges of the cylindrical wall. All nozzle flow was captured and reversed for all reverser configurations tested.

Effect of Spacing on Flow and Noise Indication

The results obtained from the flow apparatus in determining the proper spacing for the reversers are presented in table II and figure 8. The effect of spacing on flow is shown as a reverser flow parameter W/W_∞ plotted against spacing-to-nozzle-diameter ratio x/D_n. The reverser flow parameter is defined as the ratio of flow rate with the reverser to flow rate without the reverser at the same nozzle pressure ratio. The noise indication from the 20-kilohertz scale of the portable noise meter is also plotted against the spacing-to-nozzle-diameter ratio.

The results for both cylindrical reversers with the 5.24-centimeter-diameter nozzle are shown in figure 8(a). There is no difference in the effect of spacing between the two cylindrical reversers, either on flow or noise indication. The effect of spacing on flow does not start until after the reverser overlaps the nozzle exit, that is for values of x/D_n less than 0. The noise meter readings, however, indicated a significant decrease (5 dB) in noise level when the spacing ratio was decreased from 0.6 to 0.3. Above x/D_n of 0.6 the noise level did not change appreciably. At low values of x/D_n, which affected the flow, the noise level decreased slightly, possibly reflecting the change in flow. For reference, the line labeled "point of contact" is the location at which the nozzle inside diameter, if projected, would contact the reverser.

There was an appreciable difference in the results obtained for the cylindrical reversers when the 7.78-centimeter-diameter nozzle was used. Figure 8(b) shows that with this combination of nozzle and reversers, the flow is affected at a spacing ratio as large as 0.8 for both reversers. For x/D_n less than 0.8, the smaller cylindrical reverser shows a bigger drop in flow ratio for a given spacing ratio. The noise indication does not show the sudden decrease in noise level without change in flow noticed in figure 8(a). The noise level reduction for x/D_n less than 0.8 seems to be the effect of the lower flow rate.

The difference in behavior between the cylindrical reversers with the 5.24- and 7.78-centimeter-diameter nozzles can be attributed to the different area ratios. As shown in table I, the area ratios A_f/A_n for both reversers with the 5.24-centimeter-diameter nozzle are large (5.63 and 7.02). For the 7.78-centimeter-diameter nozzle the area ratios are much smaller (2.55 and 3.18 for the smaller and larger semicylindrical reversers, respectively).

Results for the V-gutter reverser and 5.24-centimeter-diameter nozzle are shown in figure 8(c) for two different pressure ratios P_n/P_a of 1.70 and 1.42. The reverser spacing ratio affects the flow rate starting at a x/D_n of about 0.8. An appreciable transition in flow characteristics is apparent between x/D_n of 0.3 and 0.5. This effect, evident at both pressure ratios, occurred when the edge of the cover plate was in the same plane as the nozzle exit ($x/D_n = 0.36$). The noise meter indicated about the same noise level throughout the range of spacings that did not affect the flow. Noise levels were lower for the spacings that reduced the flow.

The results from the flow apparatus set the optimum spacing ratios for the different reverser-nozzle combinations. These optimum values were $x/D_n = 0$ for both cylindrical reversers with the 5.24-centimeter-diameter nozzle; $x/D_n = 0.85$ for the cylindrical reverser with the 7.78-centimeter-diameter nozzle; and $x/D_n = 0.85$ as well for the V-gutter reverser and 5.24-centimeter-diameter nozzle. The data showed that the minimum x/D_n for full flow increases with decreasing area ratio. In the range approaching minimum spacing for full flow, the noise decreased with decreasing spacing.

This indicates that the minimum spacing for full flow represents an optimum in terms of lower noise, as well as in terms of thrust reversal as previously indicated.

Effect of Thrust Reversal on Noise

Thrust reversers are an important source of noise, as indicated by table III and figures 9 to 12. They produce higher noise levels with less directivity than the bare-nozzle jets they deflect. The reverser noise peaks at higher frequencies than that of the nozzle alone and has near-peak noise levels over a wider frequency range. The reverser noise level appears to be a function of the sixth power of the velocity, rather than having the eighth power relation typical of subsonic jets.

The flow from the cylindrical reversers was always attached to the nozzle air supply pipe. The ninth column in table III shows the angles at which the reversed jets intersected the microphone semicircle (3.05-m radius). With the 5.24-centimeter-diameter nozzle the flow was turned approximately 170° ($\theta_j = 10^{\circ}$) for most runs. With the 7.78-centimeter-diameter nozzle the flow was turned more than 170° ($\theta_j < 10^{\circ}$) so none of the microphones were in the jet. With the reverser set in the vertical plane ($\alpha = 90^{\circ}$), the jets were not in the microphone plane.

For the V-gutter reverser, the flow was turned between 115° and 130° (θ_j of 65° to 50°, table III) as determined at the intersection of one of the jets with the microphone circle. The turned jets very nearly follow the angles of the side plates ($\theta = 45^{\circ}$). Again, for the V-gutter operating in the vertical plane ($\alpha = 90^{\circ}$), the jets were not in the microphone plane. Shown in figures 9 and 10 is a comparison between the bare nozzle and the smaller semicylindrical reverser with the 5.24-centimeter nozzle at the optimum spacing x/D_n of 0 and at a pressure ratio P_n/P_0 of 1.72.

The effects of thrust reversal on noise directivity pattern and noise level are shown in figure 9 as polar plots of overall sound pressure level (OASPL) against angular position. The bare-nozzle jet yields a maximum OASPL of 107 decibels at the 160° angle. Its directivity is very pronounced, with a difference of 12 decibels between maximum and minimum OASPL. The noise level decreases by 5 decibels over the 30° increment between the peak noise ($\theta = 160^{\circ}$) and the noise at θ of 130°. In comparison, the noise pattern for the reverser appears nearly uniform: its maximum OASPL is 113 decibels, which is 6 decibels higher than that of the bare nozzle; its minimum OASPL value is 109 decibels, which is 2 decibels higher than the maximum level for the bare nozzle. While the maximum OASPL occurs at an angle θ of 10°, there is only a 4-decibel decay in OASPL around the whole semicircle.

Figure 10 shows the effects of thrust reversal on the spectral distribution. The sound pressure level (SPL) is plotted against the 1/3-octave-band center frequency f_c at two different microphone angles (10° and 160°). These are the angles of maximum

OASPL for the reverser configuration and the nozzle only, respectively. With the bare nozzle the dominant noise occurs at a center frequency of 1250 hertz for the direction of maximum OASPL ($\theta = 160^{\circ}$), while on the back lobe (at $\theta = 10^{\circ}$) the maximum SPL appears over a broader band (between 2000 and 6300 Hz). The difference in front and back noise level at frequencies below 2000 hertz is much larger than at frequencies above 2000 hertz. For example, the difference in SPL at the 800-hertz 1/3-octave band is about 24 decibels, as compared with 9 decibels at 3200 hertz and 5 decibels at 8000 hertz. The effect of angular position on the noise spectrum for the reverser is much smaller, as was the directivity pattern. The differences in SPL for the two angular positions are fairly uniform over the whole frequency range, and the peak frequencies change only from 8000 hertz to 5000 hertz. It should be noted that for the bare nozzle the peak frequency shifts to higher values as the angle shifts away from the maximum OASPL direction, whereas with the reverser the shift is in the opposite direction (the peak frequency becomes lower). The shape of the bare-nozzle-only spectrum at θ of 10° (fig. 10) is similar to the reverser curves at θ of 10° and 160° but is lower by 16 decibels.

The variation in maximum OASPL with velocity is shown in figure 11. This figure includes all the reverser combinations tested at their optimum spacing ratio. In addition, the bare-nozzle datum point is included for comparison. The noise level data for all the reversers at optimum spacing follow a sixth-power-of-velocity relation very closely. All the cylindrical reverser configurations fall nearly on the same line. The V-gutter noise level is approximately 6 decibels higher. For the same operating conditions the magnitude of the maximum OASPL was about the same, whether measured on the plane of the jet flow or at 90° to it.

An eighth-power relation, as indicated in reference 18, was drawn through the bare-nozzle datum point. This indicates that at 294-meter-per-second velocity the quietest of the target-type reversers has a maximum OASPL 6 decibels higher than that of the bare nozzle. At lower velocities this difference increases due to the slopes of the sixth- and eighth-power relations.

These same data are replotted in figure 12 in terms of effective overall power level (OAPWL). The effect is the same as with the maximum overall sound pressure level: the overall power level for the target-type reversers is a function of the sixth power of the jet velocity leaving the nozzle. The plots differ only in that at the 294-meter-per-second velocity the difference in OAPWL between the bare nozzle and the quietest reverser is now approximately 11 decibels. The larger difference in OAPWL as compared to the maximum OASPL is the result of the integration of the near-uniform noise directional pattern of the reversers as opposed to the highly directional pattern of the bare-nozzle jet.

The OAPWL is only a measure of true sound power level for an omni-directional sound source. The values of OAPWL obtained by integrating the sound pressure level

in the same plane or at 90° to the direction of the jets agree with each other. Minor differences are discussed in the following section.

Effect of Thrust Reverser Variables Upon Noise Directivity Patterns

The results of various thrust reverser variables examined (pressure ratio (velocity), type of target, area ratio, orientation, and spacing) are shown in figures 13 to 20 as plots of OASPL against angular position. The most important result obtained through the range of variables examined is the near-uniform noise pattern produced by target-type reversers, provided that the nozzle flow is not affected by the reversers. These variables are discussed individually.

Effect of pressure ratio on noise directivity. - The noise directivity pattern at optimum spacing for the smaller semicylindrical reverser and the 5.24-centimeter-diameter nozzle is shown in figure 13(a) at three values of nozzle pressure ratio. The equivalent data for this reverser and the 7.78-centimeter-diameter nozzle are shown in figure 13(b), and those for the V-gutter reverser and the 5.24-centimeter-diameter nozzle in figure 13(c). In none of these cases is there any variation in the noise directivity pattern with a change in pressure ratio (or nozzle jet velocity). The data for the larger semicylindrical reverser and the 5.24-centimeter-diameter nozzle are not shown, as under all conditions its performance was identical (within 1 dB) to that of the smaller semicylindrical reverser with the 5.24-centimeter-diameter nozzle.

Effect of area ratio on noise directivity. - The effect of area ratio on directivity is minor for the semicylindrical reversers. Comparison of figures 13(a) and (b) shows this effect for the smaller semicylindrical reverser. For both cases the minimum OASPL occurs on the back lobe of the reverser. The maximum OASPL occurs at θ of 10° and 30° for A_f/A_n of 5.63 and 2.55, respectively. However, the significance of this shift is obscured by the fact that the microphone at 10° is in the jet path for the case where A_f/A_n is 5.63.

Effect of orientation on noise directivity. - The effect of thrust reverser orientation on the noise pattern was checked by rotating the reversers 90° with respect to the microphone-nozzle plane. This was done for both the smaller semicylindrical and V-gutter reversers using the 5.24-centimeter-diameter nozzle. The maximum OASPL and total power (OAPWL) were the same with the reversed flow at α of 0° or 90°. This was shown in figures 11 and 12. The noise directivity patterns were altered as shown in figures 14(a) and (b). The biggest change was in the location of the maximum OASPL.

Figure 14(a) shows that the maximum OASPL for the smaller semicylindrical reverser shifted from a microphone angle θ of 10° with the jets in the same plane as the microphones ($\alpha = 0^{\circ}$) to 50° for the jets blowing in a plane at a right angle to the micro-

phone plane ($\alpha = 90^{\circ}$).

The effect of orientation α for the V-gutter reverser is shown in figure 14(b). A similar shift occurred, with the maximum OASPL moving from $\theta = 10^{\circ}$ to $\theta = 50^{\circ}$. In addition, a change in distribution occurred on the back lobe, causing the minimum OASPL to shift from $\theta = 80^{\circ}$ for the 0° orientation to $\theta = 160^{\circ}$ for the 90° case. In effect, for the jets in a plane at 90° to the microphones the directivity patterns of the smaller semicylindrical and V-gutter reversers were very similar.

It should be kept in mind that these changes are relatively small and that in either plane the directivity pattern is very uniform when compared to the bare jet.

Effect of reverser spacing on noise directivity. - The noise meter readings from the runs made in the flow apparatus, presented in table II and figure 8, showed in a qualitative way that the spacing of the reversers affected the noise levels. This effect was studied further by varying the spacing on all three reversers with the 5.24-centimeter-diameter nozzle in the acoustic facility, as shown in figure 15.

The data for the smaller and larger semicylindrical reversers are shown in figures 15(a) and (b), respectively. These two sets of data are directly comparable, as there was no difference in the performance of the semicylindrical reversers with the 5.24-centimeter-diameter nozzle. The spacing x/D_n was increased from the optimum, 0, to 1.61 (larger reverser only). Except for the screech at an x/D_n of 1.61, there was little effect of the spacing on noise level, except in the range $0.3 \leq x/D_n \leq 0.6$, where the increase in noise with increasing spacing was appreciable. In all cases, the directivity was unaffected.

For the V-gutter reverser (fig. 15(c)), the spacing was decreased from the optimum rather than increased. The changes in noise directivity patterns are pronounced. The noise levels cannot be compared directly as the total flow rate is smaller at x/D_n of 0.42 and 0.18 than at the optimum x/D_n of 0.85. Extrapolated by a sixth-power law on the basis of equal flows, the noise level for the 0.18 spacing ratio would be higher than for the optimum point. The difference between maximum and minimum OASPL's for the $x/D_n = 0.18$ configuration is about 11 decibels, and it peaks at 20° to 30° from the direction of the emerging jets.

Effect of Thrust Reverser Variables on Noise Spectra

The spectral values of sound pressure level (SPL) at a 3.05-meter radius as well as the integrated values of effective sound power level (PWL), are listed in table IV for all the configurations tested. Figure 16 shows graphically the effects of thrust reversers upon the spectral distribution of PWL. The effects of other variables on the SPL are shown in figures 17 to 22.

Effect of different types of target reversers on effective sound power level spectrum. - The spectral effective sound power levels (PWL) for three of the reverser configurations are plotted in figure 16 against the 1/3-octave-band center frequency f_c. Also shown are equivalent data for the bare nozzle. All four curves are for the same nozzle size (5.24 cm diam) and pressure ratio P_n/P_a (1.72). The reversers have a much higher sound power level than the bare nozzle. This difference becomes larger at the higher frequencies. Of the three reverser configurations shown, the smaller semicylindrical reverser at optimum spacing has the lowest PWL, followed by the same reverser at larger-than-optimum spacing ($x/D_n = 0.6$). The V-gutter has the highest PWL of the three reverser configurations shown, even though at optimum spacing.

Effect of pressure ratio, area ratio, and shape on sound pressure level spectrum. - The effect of pressure ratio (or velocity) on the SPL at a 3.05-meter radius at optimum spacing is shown in figures 17 and 18. In all these figures the frequencies for cancellations and reinforcements due to ground reflections assuming a point source are labeled on the abscissa as C_1, C_2, C_3 and R_1, R_2, respectively.

Figure 17(a) shows the SPL spectra for the smaller semicylindrical reverser and the 5.24-centimeter-diameter nozzle at a θ of 10°, the direction of maximum OASPL for this configuration. At this angular position an additional reinforcement seems to appear in the 2.5-kilohertz 1/3-octave band. This frequency yields the apparent maximum SPL for the two lower nozzle pressure ratio curves. If the peaks at 2.5 kilohertz are disregarded, the frequency for peak SPL does not appear to shift much with pressure ratio (velocity). However, as the velocity decreases, the peak SPL is flattened out. Figure 17(b) shows the SPL for the same three cases but at a θ of 50°. The ground effects at f_c less than 1.25 kilohertz are the same for $\theta = 50^\circ$ as for $\theta = 10^\circ$. However, the effect noted at an f_c of 2.5 kilohertz is not present here. Actually, the data in table IV show that only two angular locations θ indicate this apparent reinforcement, 10° and 160°. The frequency for maximum SPL decreases with decreasing pressure ratio (velocity), from 6.3 kilohertz to 2 kilohertz at P_n/P_a of 1.72 and 1.25, respectively, as Strouhal-number reasoning would predict. These peaks agree also with the frequencies at which the PWL are maximum, as shown in table III.

The pressure ratio effects on spectral distribution of SPL are shown in figure 18(a) for the smaller semicylindrical reverser and the 7.78-centimeter-diameter nozzle at optimum spacing and a θ of 30°, the direction of maximum OASPL. The peak frequency f_m shifted from 2 kilohertz at $P_n/P_a = 1.36$ to 1.2 kilohertz at $P_n/P_a = 1.17$. This change is almost directly proportional to the velocity change, which would make it agree qualitatively with the Strouhal relation ($S_{max} = f_m D_n/V_n$).

The SPL spectra for the V-gutter and the 5.24-centimeter-diameter nozzle at optimum spacing ($x/D_n = 0.85$) at three pressure ratios (velocities) are shown in figure 18(b) for the maximum OASPL angle ($\theta = 10^\circ$). The spectral distribution is considerably dif-

ferent from that of the semicylindrical reversers. The SPL rises more steeply at the lower frequencies but falls more slowly at higher frequencies. The reinforcement previously apparent at an f_c of 2.5 kilohertz in the $\theta = 10^o$ direction is not present. The frequency for maximum SPL is constant at the 1.25-kilohertz band, apparently unaffected by velocity. Nor was this a directional effect; this peak appeared at all microphone locations. No "screech" was evident either.

Effect of orientation on SPL spectrum. - The effect of reverser orientation upon the spectral distribution of SPL is shown in figures 19(a) and (b) for the smaller semicylindrical reverser with the 5.24-centimeter-diameter nozzle. This effect is shown as a comparison of the spectrum at two different pressure ratios for the reverser exiting jets in the plane of the microphones ($\alpha = 0^o$) and the exiting jets at 90^o to the microphone plane ($\alpha = 90^o$). Figure 19(a) presents the comparison for the angular position where the maximum OASPL occurs for the reversed jets blowing in the microphones plane ($\theta = 10^o$). Figure 19(b) is the comparison at the angle of maximum OASPL for the jets blowing at 90^o to the microphone plane ($\theta = 50^o$). The variations in SPL which cause the shift in maximum OASPL from 10^o to 50^o with change in reverser orientation are shown to occur only at high frequencies ($f > 1.6$ kHz). The lower frequency range is unaltered by the shift in orientation. The apparent reinforcement at an f_c of 2.5 kHz still appears at the 10^o direction even with the rotated reverser. For the $\alpha = 90^o$ orientation, the frequency for peak SPL does not seem to shift with pressure ratio (velocity) at the maximum OASPL direction ($\theta = 50^o$). It shifts appreciably at the 10^o microphone angle if the apparent reinforcement at 2.5 kHz is discounted. These results are the same as those obtained with the reverser blowing in the plane of the microphones. There is actually no difference in the effective sound power level spectrum (PWL) and effective overall sound power level (OAPWL) obtained by assuming either set of SPL values as constant over the corresponding portions of the integrating surface.

The effect of orientation of the V-gutter reverser with the 5.24-centimeter-diameter nozzle is shown in figures 20(a) and (b). The comparison is made between the exiting jets at 90^o to the microphone plane ($\alpha = 90^o$) and the jets in the microphone plane ($\alpha = 0^o$) at a pressure ratio of 1.72. Figure 20(a) compares the results at the direction of maximum OASPL for the $\alpha = 90^o$ orientation ($\theta = 50^o$). Figure 20(b) shows the comparison at the direction of maximum OASPL for the $\alpha = 0^o$ orientation ($\theta = 10^o$). For this reverser it appears that changes occur throughout the spectrum. The effects in magnitude of SPL are largest at frequencies above 1.0 kilohertz. At frequencies below 1.0 kilohertz the effects are complicated by apparent changes in the effects of ground reflections. Such changes are not surprising as the exiting jets from the reversers leave at 45^o from the axis and one jet is aimed at the ground.

Effect of spacing on sound pressure level spectrum. - An increase in spacing from the optimum spacing increased the noise level on the smaller semicylindrical reverser

with the 5.24-centimeter-diameter nozzle. This is shown in figure 21(a) for three different spacing ratios x/D_n: 0 (optimum), 0.30, and 0.61 for otherwise equal conditions. The change in SPL from 0 to 0.30 was small; the change from 0.30 to 0.61 was larger. There was no significant change at frequencies above 8 kilohertz, and only a slight increase in SPL at frequencies below 1 kilohertz. The bulk of the change in SPL occurred between 1 and 6.3 kilohertz. The center frequency for peak SPL decreased with an increase in spacing (from 6.3 kHz at $x/D_n = 0$ to 2.0 kHz at $x/D_n = 0.61$).

The effect on the larger semicylindrical reverser with the 5.24-centimeter-diameter nozzle as the spacing ratio x/D_n was increased from 0 (optimum) to 0.61 was the same, as shown in figure 21(b). The SPL's in the frequency range of 1.0 to 6.3 kilohertz increased appreciably with increase in spacing, yet practically no change was noted above 8 kilohertz and the change was small below 1.0 kilohertz. The shift in peak frequency was similar to that of the smaller semicylindrical reverser. However, an attempt to increase the spacing to 1.61 produced an appreciable "screech." The only real difference between the spectrum for 0.61 and 1.61 is at the 2.0-kilohertz 1/3 octave band. A narrow-band analysis of this frequency range was made, as shown in figure 22, and indicated the presence of a discrete tone at 2.20 kilohertz.

Sideline Noise for Typical Full-Scale STOL Application

A calculated SPL spectrum for a reverser for a typical full-scale augmentor-wing STOL airplane, such as discussed in references 19 and 20, is shown in figure 23. The figure shows the noise spectrum for four 65.5-centimeter-diameter nozzles in parallel at a 152.5-meter sideline position and a cold jet velocity of 295 meters per second. The solid line is the spectrum for the four nozzles with reversers. The dotted line is the spectrum for the four nozzles without reversers. These nozzles and velocities are in the range of jet core magnitudes necessary for a 45 400-kilogram (100 000-lb) STOL aircraft at landing approach condition. The perceived noise level (PNL) was calculated from this spectral data using the procedure of SAE ARP 865A (ref. 20). It is obvious that the estimated 112-PNdB noise level with reversers will present a noise problem, as it is well above the design goal of 95-PNdB sideline noise at 152.5 meters (500 ft). It is also 11 decibels louder than that obtained by scaling the bare-nozzle data.

Figure 23 was constructed by scaling $12\frac{1}{2}$ times the results of the smaller semicylindrical reverser with the 5.24-centimeter-diameter nozzle. The spectral distribution was assumed to scale in a Strouhalian manner. The effect of the four engines was accounted for by increasing the single-engine noise level by 6 decibels. Proper atmospheric attenuation values were applied at the scaled frequencies. The scaling of results

$12\frac{1}{2}$ times introduced an uncertainty in noise levels at frequencies above 1.6 kilohertz. Above this frequency SPL's were obtained by extrapolation.

The variation of PNL along the 152.5-meter sideline as a function of distance behind the hypothetical aircraft is shown in figure 24. Because of the different directivity patterns of the jet noise and the reverser noise, the position where the peak noise occurs at the 152.5-meter sideline position shifts. For the reverser it occurs ahead of the aircraft; for the bare jet it occurs behind the aircraft. As figure 24 shows, a greater distance along the sideline will be subjected to high noise levels at any one time for the reversers than would be the case for a plain jet. This increase will tend to make the reverser noise even more objectionable than the 11-decibel increase in PNdB above the jet noise would indicate.

Due to the uniform directivity of the reverser noise, the considerations made about sideline noise also apply approximately to flyover noise during landing approach.

SUMMARY OF RESULTS

This experimental investigation on the noise generated by target-type thrust reversers covered two types of models: semicylindrical and V-gutter. Spacings between reverser and nozzle were varied between spacing-to-nozzle-diameter ratios of 0 and 1.61. Nozzle pressure ratios ranged from 1.25 to 1.72. The main results of this investigation can be summarized as follows:

1. The small-scale semicylindrical and V-gutter target-type reversers were significantly noisier than the nozzle alone by 5 to 15 decibels. Test results when scaled up to conditions suitable for a 45 400-kilogram augmentor-wing STOL aircraft showed that noise levels would be above the present design goal of 95-PNdB sideline noise if full thrust reverse is used. This indicates that target-type thrust reversers for core flow used during STOL-flights will constitute an important noise source.

2. The noise directivity patterns for target-type reversers are very uniform. No more than 6 decibels variation in overall sound pressure level (OASPL) was encountered among all the angular directions tested, either in the plane of the exiting jets or at 90° to that plane. Maximum values of OASPL occurred between the angles of 10° to 15° from the nozzle upstream axis, depending on the particular configuration. The uniformity of the noise directivity extended to the spectral distribution. The SPL distribution throughout the spectrum was nearly the same in all directions.

3. For all reverser configurations tested, the minimum noise level for a given jet velocity occurred at the minimum spacing between nozzle and reverser that does not affect the flow rate. Decreasing the spacing from this optimum decreased the flow rate; increasing the spacing increased the noise level.

4. The maximum overall sound pressure level ($OASPL_{max}$) at optimum spacing followed a sixth-power relation to isentropic nozzle jet velocity V_n for each geometric configuration; that is, $10^{[(OASPL)_{max}]/10} \propto V_n^6$. The data for all cylindrical reversers agreed well. The V-gutter reverser was noisier than the cylindrical reversers. These results were the same with respect to the overall sound power level (OAPWL).

5. The variations in nozzle pressure ratio (velocity), area ratio, and orientation for both semicylindrical and V-gutter reversers had very little effect, if any, on noise directivity patterns. The variation in shape from semicylindrical to V-gutter reverser shifted the location of minimum OASPL from the back lobe to the sideline of the reverser. Variations in spacing above the optimum had no effect on directivity, but variations below the optimum had a marked effect on directivity.

6. No common peak Strouhal number based on nozzle size and velocity was obtained for all the reversers tested at optimum spacing. However, an increase in characteristic dimension, such as area ratio, spacing, or nozzle diameter, tended to decrease the frequency for maximum SPL for the semicylindrical reversers. The variation of peak frequency with velocity tended to be Strouhalian also. The V-gutter configuration yielded a fixed peak frequency that did not vary with velocity (for all reverser conditions that did not back pressure the nozzle).

Lewis Research Center,
National Aeronautics and Space Administration,
Cleveland, Ohio, January 10, 1972,
764-72.

APPENDIX - SYMBOLS

A_f	reverser frontal area, m^2
A_n	nozzle area, m^2
D_n	nozzle-exit diameter, m
f	frequency, Hz
f_c	1/3-octave-band center frequency, Hz
f_m	1/3-octave-band center frequency exhibiting highest sound pressure level, Hz
f_p	1/3-octave-band center frequency exhibiting highest sound power level, Hz
H	*reverser height*, m
Δh_{or}	orifice differential, m (water)
OAWPL	effective overall sound power level, dB re 10^{-13} W
OASPL	overall sound pressure level, dB re 20 $\mu N/m^2$
$(OASPL)_{max}$	maximum overall sound pressure level, dB re 20 $\mu N/m^2$
P_a	atmospheric pressure, N/m^2 abs
P_n	nozzle inlet total pressure, N/m^2 abs
P_{or}	orifice upstream pressure, N/m^2 abs
PNL	perceived noise level, PNdB
PWL	effective sound power level, dB re 10^{-13} W
S_{max}	Strouhal number at peak frequency, $f_m D_n/V_n$
SPL	sound pressure level, dB re 20 $\mu N/m^2$
T_a	ambient temperature, K
T_n	nozzle inlet temperature, K
T_{or}	orifice inlet temperature, K
V_n	nozzle jet velocity, m/sec
W	mass flow rate, kg/sec
W_∞	mass flow for nozzle with no reverser (infinite spacing), kg/sec
x	spacing between reverser and nozzle, m
Z	reverser width, m

α reverser orientation (angle of reverser to horizontal), deg

θ microphone angle from nozzle upstream axis, deg

θ_j angle from nozzle axis at which flow occurs on microphone plane, deg

θ_m angle from nozzle axis at which maximum OASPL occurs

REFERENCES

1. Sanders, Newell D.; Diedrich, James H.; Hassell, James L., Jr.; Hickey, David H.; Luidens, Roger W.; and Stewart, Warner L.: V/STOL Propulsion. Aircraft Propulsion. NASA SP-259, 1971, pp. 135-168.

2. Dorsch, R. G.; Krejsa, E. A.; and Olsen, W. A.: Blown Flap Noise Research. Paper 71-745, AIAA, June 1971.

3. Povolny, John H.; Steffen, Fred W.; and McArdle, Jack G.: Summary of Scale-Model Thrust-Reverser Investigation. NACA TR 1314, 1957.

4. McArdle, Jack G.: Performance Characteristics of Ring-Cascade-Type Thrust Reversers. NACA TN 3838, 1956.

5. Ashwood, P. F.: The Preliminary Testing of an Aerodynamic Design of Thrust Spoiler. Memo. M.138, National Gas Turbine Establishment, England, Oct. 1951.

6. Steffen, Fred W.; McArdle, Jack G.; and Coats, James W.: Performance Characteristics of Hemispherical Target-Type Thrust Reversers. NACA RM E55E18, 1955.

7. Steffen, Fred W.; and McArdle, Jack G.: Performance Characteristics of Cylindrical Target-Type Thrust Reversers. NACA RM E55I29, 1956.

8. Tolhurst, William H., Jr.; Hickey, David H.; and Aoyagi, Kiyoshi: Large-Scale Wing-Tunnel Tests of Exhaust Ingestion Due to Thrust Reversal on a Four-Engine Jet Transport During Ground Roll. NASA TN D-686, 1961.

9. Kohl, Robert C.; and Algranti, Joseph S.: Investigation of a Full-Scale, Cascade-Type Thrust Reverser. NACA TN 3975, 1957.

10. Falarski, Michael D.; and Mort, Kenneth W.: Full-Scale Wing-Tunnel Investigation of a Target-Type Thrust Reverser on the A-37B Airplane. NASA TM X-1985, 1970.

11. Kohl, Robert C.: Performance and Operational Studies of a Full-Scale Jet-Engine Thrust Reverser. NACA TN 3665, 1956.

12. Poland, Dyckman T.: The Aerodynamics of Thrust Reversers for High Bypass Turbofans. Paper 67-418, AIAA, July 1967.

13. Sutter, Joseph: Reverse Thrust for Jet Transports. SAE Trans., vol. 63, 1955, pp. 379-385.

14. Mount, J. S.; and Lawson, D. W. R.: Developing, Qualifying, and Operating Business Jet Thrust Reversers. Paper 690311, SAE, Mar. 1969.

15. Green, M. J.: Rolls-Royce Thrust Reversers - Compatability and Reliability. Paper 690410, SAE, Apr. 1969.

16. Caffier, E.: The SNECMA Thrust Reverser System of Concorde's Prototypes. Paper 690412, SAE, Apr. 1969.

17. Wood, Stuart K.; and McCoy, Joe: Design and Control of the 747 Exhaust Reverser Systems. Paper 690409, SAE, Apr. 1969.

18. Olsen, William A.; Dorsch, Robert G.; and Miles, Jeffrey H.: Noise Produced by a Small-Scale, Externally Blown Flap. NASA TN D-6636, 1972.

19. Huff, Ronald G.; and Groesbeck, Donald E.: Splitting Supersonic Nozzle Flow into Separate Jets by Overexpansion into a Multilobed Divergent Nozzle. NASA TN D-6667, 1972.

20. Anon.: Definitions and Procedures for Computing the Perceived Noise Level of Aircraft Noise. Aerospace Recommended Practice 865A, SAE, Aug. 15, 1969.

TABLE I. - NOZZLE-REVERSER SIZE RELATIONS

Thrust reverser				Nozzle		Area ratio, A_f/A_n	Height-to-nozzle-diameter ratio, H/D_n	Width-to-nozzle-diameter ratio, Z/D_n	Width-to-height ratio, Z/H
Type	Height,[a] H cm	Width,[b] Z cm	Frontal area, A_f, cm^2	Throat diameter, D_n cm	Throat area, A_n, cm^2				
Smaller semicylindrical	8.80	13.80	121.44	5.24	21.65	5.63	1.68	2.63	1.57
				7.78	47.54	2.55	1.13	1.77	1.57
Larger semicylindrical	8.80	17.20	151.36	5.24	21.65	7.02	1.68	3.28	1.95
				7.78	47.54	3.18	1.13	2.21	1.95
V-gutter	6.60	7.94	52.40	5.24	21.65	2.43	1.26	1.52	1.20

[a]Reverser height equals length of side plates at free edge.

[b]Reverser width equals distance between side plates at free edge.

TABLE II. - EXPERIMENTAL DATA ON EFFECT OF SPACING

(a) Smaller semicylindrical reverser

Spacing ratio, x/D_n	Flow ratio, W/W_∞	Noise reading,[a] dB
With 5.24-cm nozzle; pressure ratio, P_n/P_a, 1.70		
1.46	0.99	131
.97	.98	132
.73	.98	133
.52	.98	133
.27	.99	129
.12	1.00	128
-.12	.99	128
-.39	.85	125
-.58	.52	[b]123
With 7.78-cm nozzle; pressure ratio, P_n/P_a, 1.4		
1.48	0.99	126
1.07	1.01	126
.76	.98	125
.50	.90	123
.27	.81	123

(b) Larger semicylindrical reverser.

Spacing ratio, x/D_n	Flow ratio, W/W_∞	Noise reading,[a] dB
With 5.24-cm nozzle; pressure ratio, P_n/P_a, 1.70		
1.55	0.99	133
1.30	.98	134
.94	↓	133
.70	↓	133
.48	↓	131
.24	1.00	126
.12	.99	127
-.03	.99	127
-.27	.94	127
-.52	.64	[b]125
With 7.78-cm nozzle; pressure ratio, P_n/P_a, 1.4		
1.53	0.99	126
1.24	1.00	125
1.05	.99	125
.74	.97	125
.50	.94	124
.27	.89	123
.11	.84	123
-.08	.73	122

(c) V-gutter reverser with 5.24-cm-diameter nozzle

Spacing ratio, x/D_n	Flow ratio, W/W_∞	Noise reading,[a] dB
Pressure ratio, P_n/P_a, 1.70		
0.98	1.01	131
.76	1.00	130
.50	.86	130
.27	.89	125
.18	.82	123
Pressure ratio, P_n/P_a, 1.4		
1.76	0.98	127
1.48	.99	127
1.24	1.00	128
.94	1.00	127
.73	.97	127
.48	.82	124
.24	.84	116
.15	.77	117

[a]20-kHz scale of portable noise meter.
[b]Slight screech or whistle.

TABLE III. - SUMMARY OF ACOUSTIC DATA

Run	Test conditions					Major results					
	Nozzle diameter, D_n, cm	Reverser (a)	Spacing ratio, x/D_n	Angle to horizontal, α, deg	Pressure ratio, P_n/P_a	Overall sound power level, OAPWL, dB re 10^{-13}W	Frequency for maximum power level, f_p, Hz	Flow angle at microphone plane, θ_j, deg	Maximum overall sound pressure level, $(OASPL)_{max}$, dB re 20 $\mu N/m^2$	Angle for maximum OASPL, θ_m, deg	Frequency for maximum sound pressure level at θ_m, f_m, Hz
1	5.24	None	----	--	1.72	128.6	1 250	180	107.4	160	1250
2		Sm-cyl	0	0	1.72	138.6	6 300	~10	113.3	10	8000
3				0	1.42	132.6	4 000	~10	107.0	10	[b]2500
4				0	1.25	127.2	2 000	~10	101.3	10	[b]2500
5				90	1.72	139.7	6 300	0	114.5	50	6300
6				90	1.25	127.7	6 300	0	102.0	50	6300
										30	2500
7			.61	0	1.72	143.0	2 000	~10	117.4	65	2000 to 2500
8			.30		1.72	139.7	4 000	~10	113.6	10	5000 to 6300
9	7.78		.84		1.36	133.7	2 500	~0	108.4	30	1600 to 2000
10	7.78		.84		1.17	123.7	1 250	~0	97.5	30	1250
11	5.24	Lg-cyl	0		1.72	140.0	10 000	~0	114.3	10	6300
12			0		1.25	127.5	5 000	10 to 20	101.9	10	5000
13			.61		1.72	144.1	2 500	~0	118.4	65	2000
[c]14			1.61		1.72	145.5	2 000	~0	120.4	50	2000
15		V-gutter	.85		1.72	144.4	1 250	~50	120.9	10	1250
16					1.25	133.2		~65	109.9	10	
17					1.42	139.2		~50	116.0	10	
18				90	1.72	145.1		0	120.1	50	
19		None	----	--	1.72	128.9	2 000	180	107.0	160	
20		V-gutter	[d].42	0	[e]1.69	139.5	6 300	(f)	113.7	70	6300
21			[d].36		[e]2.03	144.7	2 500		119.1		2500
22			[d].27		[e]2.47	146.7	4 000		121.8		4000
23			[d].18		[e]1.59	134.3	6 300		111.2		6300

[a]Sm-cyl denotes smaller semicylindrical reverser; lg-cyl denotes larger semicylindrical reverser.

[b]Possibly affected by reinforcement.

[c]Screech at ~2200 Hz.

[d]Too small for full flow.

[e]Static pressure ratio.

[f]Not recorded.

TABLE IV. - DETAILED ACOUSTIC DATA

(a) Run 1.

Nozzle diameter, D_n, 5.24 cm	No reverser
Spacing ratio, x/D_n, --	Reverser orientation, α, ---
Pressure ratio, P_n/P_a, 1.72	Velocity, V_n, 294 m/sec
Nozzle inlet temperature, T_n, 301 K	Ambient temperature, T_a, 299 K
Ambient pressure, P_a, 99.1 kN/m^2 abs	Relative humidity, 40 percent

1/3-Octave-band center frequency, f_c, Hz	Angle from nozzle axis, θ, deg								Power level, PWL, dB re 10^{-13} W
	160	130	100	80	65	50	30	10	
	Sound pressure level, SPL, dB re 20 μN/m^2								
200	81.3	73.7	69.0	67.0	67.0	65.3	65.0	65.0	100.8
250	85.0	75.3	71.0	68.7	68.0	66.3	66.7	66.0	103.8
315	89.0	79.0	75.7	73.0	72.3	70.0	69.7	68.0	107.8
400	92.0	82.0	79.3	77.0	76.3	74.0	73.0	70.0	110.9
500	93.0	83.0	80.0	79.0	78.0	76.3	75.0	72.7	111.9
630	95.0	84.0	79.0	77.0	77.0	76.4	75.0	74.0	113.4
800	99.0	88.0	84.0	82.0	80.4	78.0	77.0	75.0	117.4
1000	98.0	87.7	83.0	82.0	81.7	81.0	79.0	78.0	116.7
1250	99.0	89.7	86.0	84.0	83.0	81.0	81.0	81.0	118.0
1600	98.1	91.1	87.1	85.1	84.1	82.4	82.1	83.4	117.9
2000	97.1	92.1	88.1	86.1	85.7	85.1	86.1	85.1	118.1
2500	95.4	92.1	88.1	86.4	86.1	85.1	85.1	84.4	117.4
3150	94.1	92.1	88.8	86.4	86.1	85.1	85.1	85.1	117.2
4000	92.1	92.1	88.8	87.1	86.1	86.1	85.1	84.5	116.9
5000	92.2	91.8	88.8	86.2	86.2	86.2	85.2	85.2	116.7
6300	90.5	91.5	88.9	86.2	86.2	86.2	85.2	84.2	116.3
8000	89.3	90.9	87.9	85.9	85.3	85.3	84.6	84.3	115.6
10000	88.3	90.0	88.0	85.3	85.3	85.3	84.3	83.3	115.1
12500	86.4	89.1	87.1	84.4	84.7	84.4	83.4	82.4	114.1
16000	83.8	88.2	86.2	84.2	83.5	83.5	81.5	80.5	113.0
20000	82.0	86.3	84.3	83.0	82.3	82.0	80.0	77.6	111.3
Overall	107.4	102.5	99.3	97.2	96.7	96.2	95.6	95.0	128.6

(b) Run 2.

Nozzle diameter, D_n, 5.24 cm	Smaller semicylindrical reverser
Spacing ratio, x/D_n, 0	Reverser orientation, α, 0^o
Pressure ratio, P_n/P_a, 1.72	Velocity, V_n, 294 m/sec
Nozzle inlet temperature, T_n, 301 K	Ambient temperature, T_a, 299 K
Ambient pressure, P_a, 99.1 kN/m^2 abs	Relative humidity, 40 percent

1/3-Octave-band center frequency, f_c, Hz	Angle from nozzle axis, θ, deg								Power level, PWL, dB re 10^{-13} W
	160	130	100	80	65	50	30	10	
	Sound pressure level, SPL, dB re 20 μN/m^2								
200	72.0	72.0	72.5	73.7	79.0	79.0	79.0	79.5	103.7
250	72.7	74.3	75.3	76.3	79.0	80.3	81.3	82.0	105.4
315	78.0	79.0	80.0	81.3	83.0	84.3	85.3	85.5	109.6
400	83.0	84.0	84.0	85.0	86.0	87.3	89.0	88.0	113.3
500	85.3	85.3	85.7	85.7	87.0	88.7	89.7	88.5	114.4
630	84.4	84.0	84.0	84.0	86.0	87.5	90.7	90.0	113.8
800	89.7	90.7	90.4	90.0	91.0	94.0	95.7	94.0	119.5
1000	92.0	91.4	90.7	90.4	91.0	93.4	94.4	93.0	119.5
1250	93.0	93.0	94.0	93.0	94.0	95.7	97.0	95.0	121.9
1600	94.7	93.1	94.1	95.1	96.1	96.7	97.7	97.1	122.9
2000	97.4	96.1	97.1	97.4	99.1	99.7	99.1	98.6	125.5
2500	99.1	97.7	99.1	100.1	101.1	101.4	102.1	103.1	127.8
3150	98.4	98.8	100.4	101.1	103.1	102.8	102.8	102.1	128.8
4000	99.8	99.5	101.1	101.5	102.1	102.8	102.8	103.1	129.0
5000	100.2	99.5	101.2	100.8	102.2	102.8	103.2	103.7	129.1
6300	99.2	99.2	102.2	102.2	103.2	103.2	104.2	104.2	129.8
8000	98.6	99.3	101.6	102.3	103.3	103.3	103.6	105.3	129.6
10000	97.3	98.7	101.3	101.3	102.3	102.3	103.0	104.8	128.9
12500	96.4	97.4	100.7	100.1	100.4	101.1	100.7	102.4	127.6
16000	94.5	96.2	98.8	99.2	99.5	99.2	98.5	99.0	126.0
20000	93.0	94.3	96.6	97.6	97.6	97.0	96.0	96.1	124.0
Overall	109.0	109.0	111.1	111.3	112.3	112.6	112.9	113.5	138.9

TABLE IV. - Continued. DETAILED ACOUSTIC DATA

(c) Run 3.

Nozzle diameter, D_n, 5.24 cm	Smaller semicylindrical reverser
Spacing ratio, x/D_n, 0	Reverser orientation, α, 0^o
Pressure ratio, P_n/P_a, 1.42	Velocity, V_n, 238 m/sec
Nozzle inlet temperature, T_n, 301 K	Ambient temperature, T_a, 299 K
Ambient pressure, P_a, 99.1 kN/m^2 abs	Relative humidity, 40 percent

1/3-Octave-band center frequency, f_c, Hz	Angle from nozzle axis, θ, deg								Power level, PWL, dB re 10^{-13} W
	160	130	100	80	65	50	30	10	
	Sound pressure level, SPL, dB re 20 μN/m^2								
200	69.5	70.0	70.0	70.7	71.0	71.7	73.3	73.7	98.6
250	69.5	70.7	72.0	73.3	74.3	75.0	77.0	77.0	101.1
315	74.7	76.0	76.7	77.7	78.7	79.3	81.0	81.0	105.6
400	79.3	80.0	80.7	81.3	82.0	83.7	85.0	84.7	109.5
500	81.7	82.0	81.3	81.3	82.0	84.0	86.3	85.0	110.4
630	80.0	80.0	79.4	79.4	80.4	82.7	85.4	85.0	108.9
800	86.0	87.0	86.4	86.0	86.0	87.7	91.0	89.0	114.9
1000	88.0	86.7	86.7	86.0	86.0	87.0	89.0	87.0	114.6
1250	88.0	88.0	88.4	89.4	90.0	90.7	92.0	90.0	117.1
1600	90.7	90.1	90.1	91.7	92.7	93.1	93.1	92.1	119.2
2000	93.1	92.1	92.4	93.7	95.1	96.1	95.1	93.4	121.5
2500	94.1	92.1	94.4	95.1	96.1	97.1	97.1	98.1	122.8
3150	93.4	93.1	95.1	95.1	96.1	96.8	96.4	97.1	122.9
4000	93.1	93.1	95.1	95.8	96.1	96.8	96.8	97.1	123.0
5000	94.2	93.8	94.5	94.8	95.8	96.5	96.2	97.5	122.8
6300	93.2	93.2	95.2	95.5	96.2	96.2	96.9	97.2	122.9
8000	91.9	92.9	94.9	95.3	95.3	95.6	95.9	97.9	122.4
10000	90.3	91.3	94.3	94.3	94.3	94.3	94.0	96.3	121.3
12500	88.4	89.7	93.1	92.7	92.4	92.7	91.4	93.4	119.6
16000	86.5	88.2	91.2	90.8	90.5	90.8	89.5	89.5	117.7
20000	84.6	86.6	88.6	89.3	88.6	88.0	86.6	86.6	115.5
Overall	103.2	103.1	104.8	105.2	105.7	106.3	106.3	107.0	132.6

(d) Run 4.

Nozzle diameter, D_n, 5.24 cm	Smaller semicylindrical reverser
Spacing ratio, x/D_n, 0	Reverser orientation, α, 0^o
Pressure ratio, P_n/P_a, 1.25	Velocity, V_n, 192 m/sec
Nozzle inlet temperature, T_n, 299 K	Ambient temperature, T_a, 299 K
Ambient pressure, P_a, 99.1 kN/m^2 abs	Relative humidity, 40 percent

1/3-Octave-band center frequency, f_c, Hz	Angle from nozzle axis, θ, deg								Power level, PWL, dB re 10^{-13} W
	160	130	100	80	65	50	30	10	
	Sound pressure level, SPL, dB re 20 μN/m^2								
200	65.7	65.0	66.0	67.0	67.0	68.0	68.7	70.3	94.5
250	65.7	66.0	68.0	68.3	69.7	71.0	72.0	73.3	96.7
315	71.0	72.0	73.0	73.3	74.0	75.3	77.0	78.0	101.6
400	75.3	76.3	76.0	77.0	77.3	79.7	81.3	82.0	105.5
500	77.0	78.0	77.3	77.0	77.7	80.0	81.0	81.0	106.0
630	76.4	76.0	75.4	75.7	76.4	78.0	80.0	81.0	104.6
800	81.4	82.7	82.7	82.0	82.4	83.0	84.7	84.4	110.4
1000	82.7	81.0	82.0	82.0	82.0	82.7	83.4	83.4	109.8
1250	86.0	84.7	85.4	86.0	87.0	88.0	88.7	87.4	114.1
1600	87.1	87.1	87.7	89.1	90.1	90.1	90.1	89.1	116.3
2000	89.1	88.1	90.1	90.4	92.1	93.1	92.1	89.4	118.3
2500	89.1	87.7	89.1	89.4	90.1	91.4	92.7	93.1	117.6
3150	88.1	87.1	89.1	89.8	90.4	90.8	91.1	90.4	117.1
4000	87.5	87.1	88.8	89.1	90.1	90.5	90.5	90.5	116.7
5000	88.2	88.2	88.8	89.2	89.8	90.2	90.2	91.2	116.9
6300	87.5	87.9	89.2	89.2	90.2	89.2	90.5	91.5	116.8
8000	86.3	87.3	88.3	88.3	89.3	89.3	89.3	91.6	116.1
10000	83.7	84.3	87.0	86.3	87.3	87.0	86.7	89.7	114.0
12500	81.7	82.4	85.4	85.1	85.7	85.1	84.4	86.1	112.2
16000	79.8	80.8	83.5	83.5	84.2	83.2	81.8	83.2	110.4
20000	77.6	79.0	81.3	81.6	81.6	80.6	78.6	79.6	108.1
Overall	98.1	97.8	99.2	99.5	100.4	100.8	101.0	101.3	127.2

TABLE IV. - Continued. DETAILED ACOUSTIC DATA

(e) Run 5.

Nozzle diameter, D_n, 5.24 cm	Smaller semicylindrical reverser
Spacing ratio, x/D_n, 0	Reverser orientation, α, 90^o
Pressure ratio, P_n/P_a, 1.72	Velocity, V_n, 293 m/sec
Nozzle inlet temperature, T_n, 299 K	Ambient temperature, T_a, 299 K
Ambient pressure, P_a, 99.1 kN/m^2 abs	Relative humidity, 40 percent

1/3-Octave-band center frequency, f_c, Hz	Angle from nozzle axis, θ, deg								Power level, PWL, dB re 10^{-13} W
	160	130	100	80	65	50	30	10	
	Sound pressure level, SPL, dB re 20 μN/m^2								
200	71.3	72.0	73.0	75.0	79.0	79.0	79.0	79.0	103.8
250	72.0	74.0	77.0	78.3	80.3	80.7	81.7	82.0	106.1
315	78.0	80.3	82.3	83.7	85.0	85.0	86.0	86.0	111.0
400	83.0	85.0	86.0	87.0	88.0	88.0	89.0	89.0	114.5
500	85.0	86.7	87.7	87.7	88.7	88.7	89.7	88.0	115.5
630	84.0	84.0	84.0	85.0	87.0	87.7	90.0	90.0	113.9
800	90.0	90.0	90.0	91.0	92.0	92.4	94.0	93.4	119.0
1000	91.7	90.0	89.7	90.0	91.0	92.0	94.0	93.4	118.8
1250	92.7	92.0	93.0	93.0	94.7	95.4	96.7	95.0	121.5
1600	94.1	93.1	94.1	95.1	96.1	97.4	97.7	96.1	122.9
2000	96.1	95.1	96.1	97.1	98.1	100.1	99.7	96.1	125.0
2500	98.1	98.1	99.1	100.1	101.1	102.1	102.1	100.4	127.7
3150	99.1	100.1	101.4	101.1	102.8	104.1	103.1	99.1	129.3
4000	100.1	101.1	101.8	102.1	102.8	104.8	103.5	98.8	129.9
5000	99.8	100.5	101.8	101.8	103.2	105.2	103.2	98.5	129.9
6300	99.2	100.2	102.5	103.2	104.9	106.2	104.9	99.5	130.9
8000	98.9	100.3	103.3	103.3	104.3	105.9	103.9	99.3	130.7
10000	98.0	99.3	103.0	102.7	104.3	105.3	103.3	98.3	130.3
12500	97.1	98.4	101.4	101.4	102.7	102.7	101.4	97.1	128.6
16000	95.2	96.5	99.8	100.5	101.5	100.8	99.2	94.5	127.1
20000	93.0	94.6	98.0	98.6	99.6	99.6	96.6	91.0	125.2
Overall	109.0	109.8	111.8	112.1	113.4	114.5	113.3	109.4	139.7

(f) Run 6.

Nozzle diameter, D_n, 5.24 cm	Smaller semicylindrical reverser
Spacing ratio, x/D_n, 0	Reverser orientation, α, 90^o
Pressure ratio, P_n/P_a, 1.25	Velocity, V_n, 192 m/sec
Nozzle inlet temperature, T_n, 299 K	Ambient temperature, T_a, 299 K
Ambient pressure, P_a, 99.1 kN/m^2 abs	Relative humidity, 40 percent

1/3-Octave-band center frequency, f_c, Hz	Angle from nozzle axis, θ, deg								Power level, PWL, dB re 10^{-13} W
	160	130	100	80	65	50	30	10	
	Sound pressure level, SPL, dB re 20 μN/m^2								
200	65.0	66.7	67.7	67.7	68.3	68.7	70.3	71.3	95.6
250	65.5	67.3	69.3	70.0	71.0	72.0	73.0	74.0	97.9
315	71.0	73.0	75.0	75.3	76.0	76.0	77.0	77.3	102.7
400	76.0	77.7	78.7	79.0	79.7	80.0	81.0	81.3	106.7
500	78.0	79.0	79.0	79.7	80.0	80.0	81.0	81.0	107.2
630	76.7	76.0	76.0	77.0	77.4	78.0	80.0	80.6	104.9
800	82.0	82.0	82.0	83.0	83.7	84.0	84.0	84.4	110.6
1000	83.0	81.0	82.0	82.7	83.0	83.4	83.7	82.4	110.2
1250	86.0	83.0	84.0	85.0	85.7	87.0	88.0	87.0	113.1
1600	86.4	84.7	85.1	86.1	86.7	88.1	89.1	89.4	114.2
2000	87.7	87.7	87.7	88.1	89.1	91.1	92.1	89.7	116.7
2500	88.1	88.1	90.1	90.1	91.1	91.4	93.1	92.4	118.0
3150	87.1	87.1	88.8	89.4	91.1	91.1	92.1	88.1	117.2
4000	87.1	87.1	88.8	89.8	91.1	92.1	92.1	87.5	117.4
5000	88.2	88.8	89.5	90.2	91.5	92.2	92.2	87.2	117.9
6300	87.5	89.2	91.2	91.2	92.2	93.2	92.2	86.5	118.7
8000	86.3	87.3	90.3	90.3	91.6	92.6	91.3	86.3	117.8
10000	84.3	84.7	87.3	88.3	90.3	91.0	89.3	84.3	115.8
12500	82.4	83.1	85.7	86.4	87.4	88.4	87.1	81.7	113.6
16000	80.2	81.2	84.5	85.5	86.5	85.8	84.2	78.5	112.0
20000	77.6	79.0	82.0	83.6	83.6	83.6	81.6	74.6	109.6
Overall	97.7	97.9	99.5	100.0	101.2	102.0	102.0	99.1	127.7

TABLE IV. - Continued. DETAILED ACOUSTIC DATA

(g) Run 7.

Nozzle diameter, D_n, 5.24 cm	Smaller semicylindrical reverser
Spacing ratio, x/D_n, 0.61	Reverser orientation, α, 0^o
Pressure ratio, P_n/P_a, 1.72	Velocity, V_n, 293 m/sec
Nozzle inlet temperature, T_n, 299 K	Ambient temperature, T_a, 299 K
Ambient pressure, P_a, 99.1 kN/m^2 abs	Relative humidity, 40 percent

1/3-Octave-band center frequency, f_c, Hz	Angle from nozzle axis, θ, deg								Power level, PWL, dB re 10^{-13} W
	160	130	100	80	65	50	30	10	
	Sound pressure level, SPL, dB re 20 μN/m^2								
200	74.3	74.3	79.3	79.3	79.0	79.7	79.7	80.7	106.1
250	74.3	75.7	79.3	79.7	80.3	81.3	83.0	83.7	107.4
315	80.7	82.0	83.7	84.0	84.7	85.7	87.0	87.7	111.9
400	85.0	86.0	87.7	88.0	88.7	89.3	91.0	91.0	115.8
500	87.0	88.0	89.0	89.0	89.7	90.7	91.7	90.3	117.0
630	87.0	86.0	87.4	88.0	89.0	89.7	92.0	91.4	116.2
800	92.7	93.0	95.0	95.0	96.0	96.7	98.0	96.4	123.0
1000	95.0	94.0	95.0	95.4	96.0	96.4	97.0	96.0	123.1
1250	98.0	99.0	100.4	101.4	101.7	101.4	102.0	102.4	128.3
1600	100.1	102.4	106.1	106.1	107.1	106.1	105.4	104.4	132.9
2000	101.7	103.1	107.1	108.7	110.1	110.1	107.7	104.4	135.2
2500	102.4	104.1	106.1	108.1	110.1	109.4	108.4	110.1	135.0
3150	103.1	103.1	105.1	106.1	108.1	108.1	107.8	109.1	133.8
4000	102.1	103.1	104.1	105.1	107.1	107.8	107.8	107.5	133.2
5000	101.2	101.2	103.2	103.5	105.2	106.2	106.2	106.5	131.6
6300	99.9	99.5	103.2	103.2	105.2	105.5	105.5	106.2	131.2
8000	98.3	98.3	102.3	102.3	104.3	104.3	104.3	105.3	130.1
10000	97.3	97.3	101.3	101.3	103.3	103.0	102.3	104.3	129.0
12500	96.4	96.4	100.4	100.4	102.1	101.4	100.4	102.4	127.7
16000	94.2	94.5	99.2	99.5	100.5	99.5	98.2	99.5	126.1
20000	92.3	93.6	97.3	98.6	99.0	98.3	96.0	96.0	124.6
Overall	111.3	111.8	114.9	115.8	117.4	117.3	116.6	117.0	143.0

(h) Run 8.

Nozzle diameter, D_n, 5.24 cm	Smaller semicylindrical reverser
Spacing ratio, x/D_n, 0.30	Reverser orientation, α, 0^o
Pressure ratio, P_n/P_a, 1.72	Velocity, V_n, 293 m/sec
Nozzle inlet temperature, T_n, 299 K	Ambient temperature, T_a, 299 K
Ambient pressure, P_a, 99.1 kN/m^2 abs	Relative humidity, 40 percent

1/3-Octave-band center frequency, f_c, Hz	Angle from nozzle axis, θ, deg								Power level, PWL, dB re 10^{-13} W
	160	130	100	80	65	50	30	10	
	Sound pressure level, SPL, dB re 20 μN/m^2								
200	73.3	73.3	79.0	79.0	79.0	79.0	80.0	80.0	105.8
250	76.0	74.0	79.0	79.0	79.3	80.0	82.0	82.7	106.6
315	79.3	79.3	82.0	82.3	83.7	84.0	86.0	86.7	110.4
400	83.0	84.0	85.0	86.0	87.0	88.0	89.0	89.3	113.9
500	85.3	86.0	86.7	87.0	87.3	89.0	90.0	89.3	115.1
630	84.4	84.0	85.0	85.0	86.0	88.0	90.0	90.7	114.0
800	90.0	91.0	91.0	91.0	92.0	93.7	96.0	96.0	120.0
1000	93.0	92.0	93.0	92.7	92.0	93.0	95.7	94.0	120.7
1250	94.0	93.4	95.0	95.7	96.0	97.0	98.0	97.7	123.3
1600	96.1	97.1	98.1	99.1	99.7	99.7	100.1	101.1	126.2
2000	98.1	99.1	101.7	102.4	103.1	103.4	102.1	100.1	129.3
2500	99.1	99.1	102.4	103.4	104.4	104.7	103.1	104.1	130.3
3150	99.1	99.4	102.8	103.8	104.1	104.1	103.1	104.1	130.3
4000	99.1	100.1	102.8	104.1	104.1	104.1	104.1	104.1	130.6
5000	100.2	99.5	101.8	102.2	103.2	103.2	103.2	104.2	129.6
6300	99.2	99.2	101.9	102.2	103.2	103.2	104.2	104.2	129.7
8000	98.3	99.3	101.3	101.3	102.6	102.6	102.6	103.6	129.0
10000	96.3	98.0	101.0	100.3	101.3	101.5	101.0	102.3	127.9
12500	95.4	96.4	99.4	99.1	99.4	99.4	99.4	100.4	126.3
16000	93.5	94.8	98.2	98.2	98.5	98.5	97.5	97.5	125.0
20000	91.6	93.0	96.3	96.6	96.6	96.6	95.3	94.6	123.2
Overall	108.9	109.4	112.1	112.6	113.3	113.4	113.1	113.6	139.7

TABLE IV. - Continued. DETAILED ACOUSTIC DATA

(i) Run 9.

Nozzle diameter, D_n, 7.78 cm	Smaller semicylindrical reverser
Spacing ratio, x/D_n, 0.84	Reverser orientation, α, 0^o
Pressure ratio, P_n/P_a, 1.36	Velocity, V_n, 225 m/sec
Nozzle inlet temperature, T_n, 305 K	Ambient temperature, T_a, 299 K
Ambient pressure, P_a, 99.1 kN/m^2 abs	Relative humidity, 40 percent

1/3-Octave-band center frequency, f_c, Hz	Angle from nozzle axis, θ, deg								Power level, PWL, dB re 10^{-13} W
	160	130	100	80	65	50	30	10	
	Sound pressure level, SPL, dB re 20 μN/m^2								
200	74.0	74.0	74.7	75.3	75.0	75.0	76.3	76.7	102.6
250	77.0	77.3	77.7	77.3	77.7	77.7	79.0	80.0	105.4
315	83.0	83.0	83.0	82.0	82.0	82.0	83.7	84.7	110.4
400	87.0	86.7	86.0	86.0	86.0	86.0	88.0	88.7	114.2
500	89.0	87.3	87.0	87.0	87.0	88.0	90.0	90.0	115.5
630	86.4	85.0	85.0	85.0	86.7	87.4	90.0	90.0	114.2
800	95.0	92.4	92.0	92.0	93.0	94.0	96.0	96.0	121.1
1000	94.7	92.0	91.0	92.0	93.0	94.0	96.0	94.4	120.8
1250	94.0	93.0	93.0	93.0	95.0	97.0	99.0	97.7	122.7
1600	93.1	93.1	93.4	94.1	96.7	99.1	100.1	97.7	123.6
2000	94.1	93.1	94.1	94.1	97.1	99.1	100.1	96.7	123.8
2500	95.1	93.1	95.1	94.4	97.1	99.1	99.7	99.4	124.1
3150	94.1	93.1	95.1	94.8	97.1	98.4	98.1	97.8	123.6
4000	93.1	92.1	94.1	95.1	96.5	97.1	96.1	96.5	122.6
5000	93.5	92.2	94.2	94.2	96.2	96.2	94.2	96.2	122.1
6300	92.2	91.2	93.2	94.2	96.2	95.9	93.2	94.2	121.5
8000	90.6	90.3	92.3	93.3	94.9	94.3	92.3	92.6	120.3
10000	89.7	89.7	92.3	92.3	94.3	93.3	91.0	91.3	119.7
12500	88.4	88.7	91.4	91.4	93.1	91.7	89.4	89.1	118.5
16000	87.2	87.2	90.8	90.5	91.5	90.5	88.2	87.2	117.4
20000	85.6	85.6	88.6	89.3	89.6	88.6	85.6	84.0	115.6
Overall	104.9	103.7	105.0	105.2	107.1	108.1	108.4	107.6	133.7

(j) Run 10.

Nozzle diameter, D_n, 7.78 cm	Smaller semicylindrical reverser
Spacing ratio, x/D_n, 0.84	Reverser orientation, α, 0^o
Pressure ratio, P_n/P_a, 1.17	Velocity, V_n, 164 m/sec
Nozzle inlet temperature, T_n, 304 K	Ambient temperature, T_a, 299 K
Ambient pressure, P_a, 99.1 kN/m^2 abs	Relative humidity, 40 percent

1/3-Octave-band center frequency, f_c, Hz	Angle from nozzle axis, θ, deg								Power level, PWL, dB re 10^{-13} W
	160	130	100	80	65	50	30	10	
	Sound pressure level, SPL, dB re 20 μN/m^2								
200	66.7	67.0	67.7	68.0	68.0	68.7	69.3	69.7	95.6
250	70.0	69.0	69.3	70.0	70.0	71.0	71.7	71.7	97.7
315	75.7	75.0	74.7	74.7	75.0	75.3	76.0	76.7	102.8
400	80.0	79.0	78.0	78.3	79.0	79.3	80.7	80.3	106.7
500	81.7	80.0	79.0	79.3	80.0	81.3	82.0	81.3	107.9
630	79.4	78.0	77.0	77.0	78.4	79.4	81.0	80.4	106.1
800	88.4	86.0	85.4	85.0	85.4	86.4	88.0	87.4	113.9
1000	88.0	86.0	84.0	84.0	85.0	86.7	87.4	86.0	113.4
1250	87.0	85.7	85.0	85.0	86.7	88.0	89.0	87.0	114.1
1600	85.1	84.4	85.1	85.4	87.1	88.1	88.7	86.1	113.8
2000	86.1	85.1	85.1	85.4	87.1	88.1	88.1	84.4	113.8
2500	85.1	84.1	84.1	84.1	86.1	87.4	87.1	83.6	112.9
3150	84.1	83.1	83.8	83.8	85.1	86.1	85.8	81.6	112.0
4000	82.8	81.5	83.1	84.1	85.1	85.1	84.1	79.6	111.2
5000	81.8	81.2	82.2	82.5	84.2	84.2	82.2	78.7	110.1
6300	80.2	80.5	81.5	82.2	83.2	83.2	81.5	77.7	109.4
8000	79.3	79.6	81.3	81.6	82.3	82.3	80.3	76.8	108.6
10000	78.7	79.3	81.3	81.0	81.7	81.0	79.3	75.8	108.1
12500	78.1	78.7	81.7	80.4	80.7	79.7	78.7	74.4	107.7
16000	76.5	78.2	81.8	80.2	79.5	79.5	77.5	73.0	107.2
20000	74.3	76.0	78.6	77.6	77.6	76.6	74.6	70.6	104.6
Overall	96.3	95.2	95.4	95.4	96.6	97.4	97.5	95.2	123.7

TABLE IV. - Continued. DETAILED ACOUSTIC DATA

(k) Run 11.

Nozzle diameter, D_n, 5.24 cm	Larger semicylindrical reverser
Spacing ratio, x/D_n, 0	Reverser orientation, α, 0^o
Pressure ratio, P_n/P_a, 1.72	Velocity, V_n, 296 m/sec
Nozzle inlet temperature, T_n, 306 K	Ambient temperature, T_a, 299 K
Ambient pressure, P_a, 99.1 kN/m^2 abs	Relative humidity, 40 percent

1/3-Octave-band center frequency, f_c, Hz	Angle from nozzle axis, θ, deg: 160	130	100	80	65	50	30	10	Power level, PWL, dB re 10^{-13} W
	Sound pressure level, SPL, dB re 20 μN/m^2								
200	73.3	73.3	74.0	80.0	80.0	80.0	80.0	81.0	105.6
250	75.3	75.7	77.0	80.0	80.0	80.7	81.7	83.7	106.7
315	81.0	82.0	82.7	84.0	84.0	85.0	85.7	86.0	111.3
400	84.0	85.3	86.3	87.7	87.7	87.7	88.0	87.3	114.4
500	85.0	85.3	86.0	87.0	86.7	88.0	88.7	87.3	114.3
630	84.4	84.0	84.0	85.0	86.0	86.4	89.0	88.4	113.2
800	90.4	91.0	91.4	92.0	92.0	92.0	94.7	93.7	119.6
1000	92.0	91.0	92.0	92.0	92.0	92.0	94.0	93.4	119.8
1250	93.0	93.0	94.0	95.0	95.7	96.0	97.0	96.4	122.5
1600	94.1	95.1	96.1	97.1	97.4	98.1	98.1	98.4	124.3
2000	96.7	96.4	97.4	98.1	99.1	100.1	100.1	99.1	125.9
2500	98.4	97.1	99.1	100.1	101.4	101.7	101.4	103.1	127.7
3150	98.4	98.1	101.1	102.1	104.1	103.8	103.1	103.1	129.5
4000	99.5	99.1	101.1	103.1	104.1	103.1	103.1	103.1	129.7
5000	99.2	100.2	102.2	103.2	104.2	103.2	103.5	104.2	130.1
6300	99.2	100.2	103.2	104.2	105.2	103.9	104.9	106.2	131.0
8000	98.3	99.9	104.3	103.9	105.3	103.9	104.3	105.6	131.1
10000	97.7	99.7	105.0	103.3	106.0	104.0	103.3	105.3	131.2
12500	96.4	97.4	101.7	102.1	103.4	102.1	101.4	103.1	128.9
16000	94.5	96.2	99.5	100.2	101.5	100.2	99.5	100.5	126.9
20000	92.6	94.3	97.6	98.6	99.3	98.6	96.6	97.3	125.0
Overall	108.7	109.3	112.4	112.9	114.2	113.3	113.3	114.3	140.0

(l) Run 12.

Nozzle diameter, D_n, 5.24 cm	Larger semicylindrical reverser
Spacing ratio, x/D_n, 0	Reverser orientation, α, 0^o
Pressure ratio, P_n/P_a, 1.25	Velocity, V_n, 193 m/sec
Nozzle inlet temperature, T_n, 302 K	Ambient temperature, T_a, 299 K
Ambient pressure, P_a, 99.1 kN/m^2 abs	Relative humidity, 40 percent

1/3-Octave-band center frequency, f_c, Hz	Angle from nozzle axis, θ, deg: 160	130	100	80	65	50	30	10	Power level, PWL, dB re 10^{-13} W
	Sound pressure level, SPL, dB re 20 μN/m^2								
200	69.0	68.0	69.0	69.0	69.3	69.3	69.0	71.3	96.6
250	68.7	68.3	69.3	70.0	70.3	70.7	72.0	73.0	97.6
315	70.3	71.7	72.3	73.0	74.0	74.0	75.3	76.3	100.8
400	75.0	76.0	76.0	77.0	77.0	78.0	79.0	79.7	104.6
500	77.0	78.0	78.0	78.0	78.3	79.0	80.0	80.0	106.0
630	75.7	75.7	76.0	76.0	77.0	77.7	79.4	80.4	104.5
800	81.0	82.0	83.0	83.0	83.0	83.7	85.0	84.7	110.7
1000	84.0	83.0	84.0	83.4	84.0	84.0	85.0	84.0	111.5
1250	85.4	85.0	86.7	87.0	87.0	88.0	89.0	88.0	114.5
1600	86.1	86.1	87.1	88.1	89.1	89.1	89.1	88.4	115.4
2000	87.1	86.1	87.4	88.1	89.1	90.1	89.1	87.4	115.7
2500	87.4	86.7	88.1	89.1	90.1	90.1	89.4	91.1	116.4
3150	87.1	87.1	88.8	89.8	90.8	90.8	89.8	89.8	116.9
4000	88.1	88.1	90.1	91.1	92.1	92.1	91.1	92.1	118.2
5000	89.5	88.5	91.2	92.2	92.8	92.8	92.2	93.8	119.1
6300	89.2	88.5	90.2	91.2	92.2	91.2	92.2	93.2	118.4
8000	87.3	87.6	89.3	89.9	90.6	89.9	90.3	92.6	117.1
10000	85.3	85.3	87.3	87.7	88.3	87.3	87.3	90.7	114.8
12500	82.4	82.7	85.7	85.4	86.4	85.4	84.7	87.1	112.6
16000	80.5	80.8	84.2	84.2	84.5	83.5	82.2	84.2	110.9
20000	78.3	79.0	81.3	81.6	81.6	81.0	79.3	80.6	108.2
Overall	98.1	97.8	99.6	100.3	101.1	101.0	100.8	101.9	127.5

TABLE IV. - Continued. DETAILED ACOUSTIC DATA

(m) Run 13.

Nozzle diameter, D_n, 5.24 cm	Larger semicylindrical reverser
Spacing ratio, x/D_n, 0.61	Reverser orientation, α, 0^o
Pressure ratio, P_n/P_a, 1.72	Velocity, V_n, 295 m/sec
Nozzle inlet temperature, T_n, 303 K	Ambient temperature, T_a, 299 K
Ambient pressure, P_a, 99.1 kN/m^2 abs	Relative humidity, 40 percent

1/3-Octave-band center frequency, f_c, Hz	Angle from nozzle axis, θ, deg								Power level, PWL, dB re 10^{-13} W
	160	130	100	80	65	50	30	10	
	Sound pressure level, SPL, dB re 20 μN/m^2								
200	77.0	80.0	80.0	80.0	80.0	80.0	80.7	81.5	107.6
250	79.3	80.0	80.3	81.0	82.0	82.5	84.0	84.3	109.1
315	82.3	84.0	84.0	85.0	85.0	86.7	87.0	87.0	112.6
400	85.0	88.0	88.7	89.0	90.0	90.3	91.0	90.0	116.7
500	88.0	89.7	91.0	91.7	92.0	92.3	92.0	90.0	118.7
630	87.4	88.4	89.0	90.0	91.0	90.7	92.0	90.7	117.5
800	95.0	97.0	99.0	99.0	99.4	99.0	99.0	97.0	126.1
1000	97.7	99.0	100.0	100.4	100.4	100.0	99.7	98.4	127.3
1250	99.0	101.0	104.0	105.0	105.0	103.7	103.0	103.0	131.1
1600	100.1	101.4	104.1	106.1	106.1	105.1	105.1	105.7	132.0
2000	103.1	105.1	107.7	109.7	111.1	111.1	109.1	105.1	136.2
2500	104.1	105.7	108.1	109.1	110.7	111.7	109.7	111.1	136.6
3150	103.1	103.1	104.8	107.1	109.1	109.1	108.4	109.1	134.4
4000	102.1	103.8	104.5	106.1	107.1	108.1	108.1	108.5	133.6
5000	101.2	101.2	103.2	105.2	106.2	106.2	106.8	108.2	132.2
6300	100.2	100.2	104.2	105.2	106.9	105.9	106.5	108.2	132.4
8000	99.3	99.6	103.3	104.3	105.9	104.9	105.3	107.3	131.4
10000	98.3	99.0	102.3	103.3	105.0	103.7	103.0	105.7	130.2
12500	97.4	97.7	101.4	101.4	103.4	102.1	101.4	103.7	128.8
16000	95.5	96.8	100.2	100.5	101.8	100.5	99.5	101.5	127.4
20000	93.6	95.3	98.3	99.6	100.3	99.6	97.0	98.3	125.9
Overall	112.1	113.3	115.7	117.1	118.4	118.3	117.5	118.2	144.1

(n) Run 14.

Nozzle diameter, D_n, 5.24 cm	Larger semicylindrical reverser
Spacing ratio, x/D_n, 1.61	Reverser orientation, α, 0^o
Pressure ratio, P_n/P_a, 1.72	Velocity, V_n, 295 m/sec
Nozzle inlet temperature, T_n, 303 K	Ambient temperature, T_a, 299 K
Ambient pressure, P_a, 99.1 kN/m^2 abs	Relative humidity, 40 percent

1/3-Octave-band center frequency, f_c, Hz	Angle from nozzle axis, θ, deg								Power level, PWL, dB re 10^{-13} W
	160	130	100	80	65	50	30	10	
	Sound pressure level, dB re 20 μN/m^2								
200	78.0	80.0	80.0	80.0	80.0	80.0	81.0	81.7	107.7
250	78.7	80.0	80.0	81.0	81.3	82.3	83.0	83.7	108.7
315	82.0	84.0	85.0	85.7	86.0	86.7	87.7	88.0	113.2
400	87.0	89.0	89.0	90.0	90.0	90.7	91.3	91.7	117.4
500	90.0	90.3	91.0	91.7	92.0	92.3	92.7	91.7	119.0
630	89.7	90.0	90.4	90.4	90.7	90.7	91.4	90.7	118.1
800	97.7	98.0	99.0	99.0	98.7	98.0	98.4	97.0	126.1
1000	99.4	99.0	100.0	100.4	100.0	100.0	100.0	99.0	127.5
1250	107.7	104.0	105.7	107.4	107.7	107.0	106.0	105.7	134.1
1600	105.7	102.7	104.4	106.4	107.4	107.1	106.1	105.7	133.2
[a] 2000	111.7	109.7	107.7	113.1	116.1	115.7	114.7	112.4	140.6
[a] 2500	108.7	108.1	106.7	110.4	113.1	114.1	112.1	112.1	138.4
3150	104.1	102.1	105.1	106.1	109.1	110.8	110.4	109.8	135.0
4000	100.1	101.1	103.1	105.8	108.1	108.1	107.1	108.5	133.1
5000	99.5	100.2	102.5	104.2	106.2	106.2	106.2	108.5	131.8
6300	97.5	98.5	101.9	104.2	106.2	105.2	105.2	108.2	131.2
8000	96.3	97.9	100.3	103.3	104.9	104.3	103.6	107.3	130.0
10000	95.3	97.3	100.3	102.3	104.0	102.3	101.3	106.3	129.0
12500	94.4	96.4	99.4	100.4	102.4	101.4	99.7	104.4	127.6
16000	92.8	95.5	98.5	100.2	101.5	100.2	97.5	102.2	126.6
20000	91.0	94.0	96.6	99.0	99.6	98.6	95.6	99.0	124.8
[a]Overall	116.0	114.6	115.1	118.0	120.3	120.4	119.3	119.4	145.5

[a]Data may be affected by screech at f ≈ 2200 Hz.

TABLE IV. - Continued. DETAILED ACOUSTIC DATA

(o) Run 15.

Nozzle diameter, D_n, 5.24 cm	V-gutter reverser
Spacing ratio, x/D_n, 0.85	Reverser orientation, α, 0^o
Pressure ratio, P_n/P_a, 1.72	Velocity, V_n, 296 m/sec
Nozzle inlet temperature, T_n, 305 K	Ambient temperature, T_a, 299 K
Ambient pressure, P_a, 99.1 kN/m^2 abs	Relative humidity, 40 percent

1/3-Octave-band center frequency, f_c, Hz	Angle from nozzle axis, θ, deg								Power level, PWL, dB re 10^{-13} W
	160	130	100	80	65	50	30	10	
	Sound pressure level, SPL, dB re 20 $\mu N/m^2$								
200	80.0	80.0	80.0	80.0	80.0	80.0	80.0	80.7	107.7
250	80.0	80.0	81.0	81.7	82.0	80.7	81.0	82.0	108.6
315	86.0	87.0	87.0	87.0	86.7	85.7	85.3	86.0	114.2
400	92.0	92.3	90.0	90.0	88.7	87.7	89.0	89.7	118.0
500	94.3	93.0	90.0	90.7	90.3	90.0	92.0	93.0	119.3
630	92.7	92.7	95.0	94.7	96.0	95.0	95.0	95.4	122.2
800	104.0	102.0	100.0	99.0	97.4	97.0	100.0	102.0	128.2
1000	105.0	101.4	100.0	98.4	98.0	98.4	100.0	102.4	128.3
1250	111.0	108.0	106.0	104.0	103.0	104.0	109.0	113.4	135.1
1600	107.1	106.7	105.4	105.1	105.1	104.4	109.4	113.1	134.3
2000	105.1	105.1	105.7	104.7	104.7	105.7	109.1	110.4	133.6
2500	105.1	104.4	105.1	103.7	104.1	105.7	108.1	109.1	133.0
3150	105.1	103.8	104.4	103.1	104.1	105.1	109.8	109.1	133.0
4000	104.8	104.8	105.8	104.1	105.1	106.8	109.5	108.5	133.6
5000	104.8	104.8	105.5	102.8	104.2	106.2	109.8	108.8	133.4
6300	104.5	105.2	105.5	103.2	104.5	106.5	109.9	108.9	133.6
8000	103.9	104.9	104.6	102.9	103.9	105.9	108.9	108.9	132.9
10000	103.3	105.0	103.7	102.3	103.3	105.3	108.0	108.7	132.4
12500	102.4	104.1	103.4	100.4	102.4	104.4	107.1	107.4	131.5
16000	101.2	103.8	102.5	100.5	100.8	103.5	105.2	105.8	130.3
20000	99.6	101.3	100.6	98.6	99.0	101.3	103.6	104.0	128.5
Overall	117.1	116.5	116.1	114.5	115.1	116.5	119.8	120.9	144.4

(p) Run 16.

Nozzle diameter, D_n, 5.24 cm	V-gutter reverser
Spacing ratio, x/D_n, 0.85	Reverser orientation, α, 0^o
Pressure ratio, P_n/P_a, 1.25	Velocity, V_n, 194 m/sec
Nozzle inlet temperature, T_n, 305 K	Ambient temperature, T_a, 299 K
Ambient pressure, P_a, 99.1 kN/m^2 abs	Relative humidity, 40 percent

1/3-Octave-band center frequency, f_c, Hz	Angle from nozzle axis, θ, deg								Power level, PWL, dB re 10^{-13} W
	160	130	100	80	65	50	30	10	
	Sound pressure level, SPL, dB re 20 $\mu N/m^2$								
200	70.0	70.0	70.3	70.7	71.3	70.7	71.0	71.3	98.2
250	71.5	72.7	73.3	73.7	73.0	72.7	72.3	73.3	100.6
315	78.0	77.7	77.0	77.7	77.0	76.7	75.7	76.3	104.8
400	82.3	81.3	80.0	81.0	80.0	79.3	79.3	80.0	108.2
500	84.0	82.3	83.3	84.3	82.7	82.3	81.7	82.0	110.7
630	83.7	84.0	86.4	85.4	86.4	84.7	84.4	85.0	112.8
800	93.0	90.7	89.4	89.0	88.7	89.7	92.4	95.0	118.3
1000	95.7	92.4	92.0	90.0	89.7	91.0	93.0	95.4	119.9
1250	101.7	98.7	96.7	96.4	98.4	100.4	103.0	106.4	127.4
1600	97.7	97.7	95.7	95.7	95.4	96.7	99.4	102.4	124.9
2000	95.1	94.7	93.4	93.4	93.7	96.1	96.7	98.1	122.4
2500	95.1	94.7	93.7	93.1	93.7	95.7	95.7	96.1	122.2
3150	93.8	92.1	92.1	91.1	92.4	94.8	95.8	96.1	120.8
4000	92.8	92.1	92.1	92.5	93.1	95.5	94.8	94.1	120.8
5000	91.8	92.2	91.5	90.5	91.5	94.5	94.8	94.5	120.1
6300	91.2	91.5	89.9	90.5	91.5	94.5	94.9	94.9	119.8
8000	89.3	90.6	88.9	89.6	90.6	93.6	93.3	93.3	118.6
10000	88.3	89.3	88.0	88.3	89.7	92.7	92.5	92.3	117.6
12500	86.4	88.4	87.1	86.7	88.4	91.4	91.4	91.1	116.4
16000	84.8	86.8	85.2	85.8	86.8	90.5	89.8	88.8	115.0
20000	82.6	84.6	83.3	84.0	84.3	88.6	88.0	86.6	113.0
Overall	106.4	105.1	103.9	103.6	104.4	106.6	107.9	109.9	133.2

TABLE IV. - Continued. DETAILED ACOUSTIC DATA

(q) Run 17.

Nozzle diameter, D_n, 5.24 cm	V-gutter reverser
Spacing ratio, x/D_n, 0.85	Reverser orientation, α, 0^o
Pressure ratio, P_n/P_a, 1.42	Velocity, V_n, 240 m/sec
Nozzle inlet temperature, T_n, 305 K	Ambient temperature, T_a, 299 K
Ambient pressure, P_a, 99.1 kN/m^2 abs	Relative humidity, 40 percent

1/3-Octave-band center frequency, f_c, Hz	Angle from nozzle axis, θ, deg								Power level, PWL, dB re 10^{-13} W
	160	130	100	80	65	50	30	10	
	Sound pressure level, SPL, dB re 20 μN/m^2								
200	70.0	70.7	71.0	72.0	73.0	72.0	80.0	80.0	101.5
250	73.3	74.7	76.3	77.0	76.3	76.0	80.0	80.0	104.2
315	81.0	82.0	82.0	82.0	81.7	80.3	80.7	80.7	109.2
400	87.0	86.0	84.3	84.7	83.0	82.0	84.0	84.0	112.4
500	89.0	86.3	85.0	88.0	86.3	86.0	86.0	86.3	114.3
630	89.0	90.0	92.7	92.0	92.7	91.7	92.0	91.7	119.3
800	99.7	97.4	96.0	95.0	94.0	95.0	98.0	100.4	124.4
1000	101.0	97.7	97.0	95.0	94.0	96.0	97.7	99.4	125.0
1250	108.0	105.0	102.7	101.7	101.7	104.4	108.0	111.7	132.8
1600	103.4	103.1	101.4	102.4	101.7	102.4	106.4	109.1	130.9
2000	100.4	100.1	99.1	99.7	99.4	101.1	103.7	105.1	128.3
2500	99.7	99.1	99.4	97.7	98.1	100.1	101.4	102.1	127.1
3150	98.3	98.1	99.1	96.8	97.8	100.1	103.4	102.1	127.0
4000	98.8	98.1	100.1	98.1	98.5	100.8	102.5	100.8	127.3
5000	97.8	98.5	99.2	96.2	97.5	99.8	102.5	101.2	126.7
6300	97.2	98.2	98.5	96.9	97.9	100.2	102.5	101.2	126.6
8000	95.6	97.6	97.3	95.9	96.9	99.3	101.6	101.3	125.7
10000	94.7	97.3	96.3	95.0	96.3	98.7	100.7	100.7	125.0
12500	93.7	96.4	95.7	93.4	95.4	97.7	100.1	99.4	124.1
16000	92.2	94.5	94.5	92.8	93.5	96.5	98.5	97.8	122.6
20000	90.3	92.6	92.6	91.0	91.0	95.0	97.0	95.3	120.8
Overall	112.3	111.2	110.5	109.5	109.7	111.7	114.5	116.0	139.2

(r) Run 18.

Nozzle diameter, D_n, 5.24 cm	V-gutter reverser
Spacing ratio, x/D_n, 0.85	Reverser orientation, α, 90^o
Pressure ratio, P_n/P_a, 1.72	Velocity, V_n, 296 m/sec
Nozzle inlet temperature, T_n, 305 K	Ambient temperature, T_a, 299 K
Ambient pressure, P_a, 99.1 kN/m^2 abs	Relative humidity, 40 percent

1/3-Octave-band center frequency, f_c, Hz	Angle from nozzle axis, θ, deg								Power level, PWL, dB re 10^{-13} W
	160	130	100	80	65	50	30	10	
	Sound pressure level, SPL, dB re 20 μN/m^2								
200	80.0	82.0	80.3	80.0	80.0	80.0	80.3	80.0	108.2
250	80.0	81.3	80.0	80.0	80.0	80.0	81.3	82.7	108.2
315	82.7	84.3	85.3	87.0	87.7	87.0	88.0	87.7	113.8
400	89.0	90.3	91.0	92.3	93.0	92.7	92.7	92.0	119.3
500	91.7	92.0	94.0	94.0	94.7	95.0	94.0	93.0	121.3
630	90.0	89.0	90.0	91.0	92.7	92.0	92.0	91.7	118.6
800	97.0	96.4	98.0	99.4	100.0	100.0	99.0	97.0	126.2
1000	101.0	99.4	100.0	101.0	101.7	102.0	101.0	101.0	128.4
1250	106.7	104.0	110.0	111.0	110.7	110.0	108.4	107.0	136.8
1600	103.4	105.4	107.1	108.1	108.1	108.1	106.1	106.7	134.5
2000	103.4	106.1	107.1	107.1	108.1	108.7	105.4	103.7	134.5
2500	104.1	105.1	106.1	106.1	107.7	108.1	106.1	104.7	133.9
3150	104.1	104.1	105.1	107.1	108.1	108.8	105.8	103.4	133.9
4000	103.1	104.5	105.1	107.1	108.1	109.5	105.5	102.5	134.0
5000	103.8	104.2	105.2	106.2	108.2	110.2	105.5	103.2	134.1
6300	102.9	103.2	105.2	106.2	108.5	110.2	105.5	102.9	134.0
8000	101.9	103.3	104.3	105.6	107.9	108.9	102.8	102.6	133.1
10000	101.7	102.3	104.3	105.3	107.3	109.0	102.8	102.7	132.8
12500	100.4	101.4	103.7	104.4	106.4	107.7	102.4	100.4	131.9
16000	99.5	100.5	102.8	103.5	105.5	107.2	101.5	100.2	131.1
20000	98.6	98.6	101.6	103.0	104.3	105.6	99.6	98.3	129.8
Overall	114.6	115.1	117.1	118.0	119.2	120.1	116.4	115.0	145.1

TABLE IV. - Continued. DETAILED ACOUSTIC DATA

(s) Run 19.

Nozzle diameter, D_n, 5.24 cm	No reverser
Spacing ratio, x/D_n, ---	Reverser orientation, α, ---
Pressure ratio, P_n/P_a, 1.72	Velocity, V_n, 291 m/sec
Nozzle inlet temperature, T_n, 293 K	Ambient temperature, T_a, 297 K
Ambient pressure, P_a, 99.1 kN/m^2 abs	Relative humidity, 45 percent

1/3-Octave-band center frequency, f_c, Hz	Angle from nozzle axis, θ, deg								Power level, PWL, dB re 10^{-13} W
	160	140	120	100	80	60	40	20	
	Sound pressure level, SPL, dB re 20 μN/m^2								
200	80.0	75.0	71.7	68.0	66.7	65.3	64.7	64.0	99.5
250	83.0	78.0	74.0	70.0	68.3	67.0	65.3	65.7	102.2
315	88.0	82.3	77.7	75.7	73.3	71.3	69.0	68.7	106.8
400	92.0	86.3	81.0	80.0	78.0	76.0	74.0	72.3	110.9
500	93.0	88.0	82.0	81.0	80.0	78.0	76.3	74.7	112.1
630	94.0	88.7	83.0	80.0	78.4	77.0	76.0	75.0	112.7
800	99.0	93.0	87.0	85.0	82.7	80.0	78.0	75.7	117.4
1000	97.4	93.0	86.7	84.4	83.7	82.0	80.7	79.0	116.6
1250	98.7	95.0	89.0	87.0	85.0	82.7	80.7	80.0	118.3
1600	98.0	95.0	90.0	88.0	86.0	83.7	82.7	82.0	118.3
2000	96.4	95.7	91.1	89.1	87.1	85.1	85.1	87.1	118.6
2500	95.1	95.1	92.1	90.1	88.1	86.1	85.1	85.4	118.5
3150	93.1	94.1	91.8	89.8	87.1	85.1	85.4	85.8	117.7
4000	93.1	93.8	91.1	90.1	88.1	86.1	86.1	85.8	117.7
5000	90.5	92.5	91.1	89.1	87.1	86.1	86.1	85.5	116.8
6300	89.2	91.2	91.2	89.2	87.5	85.5	86.2	85.5	116.4
8000	88.2	90.2	90.2	89.2	87.2	85.6	86.2	85.6	115.9
10000	86.3	88.3	89.9	88.3	87.3	84.6	86.3	84.6	115.2
12500	84.4	86.4	89.4	87.4	86.4	84.4	85.4	83.7	114.2
16000	82.8	85.5	88.1	86.5	85.5	83.8	84.5	82.5	113.2
20000	80.9	82.9	86.6	84.6	83.6	82.6	82.2	79.9	111.4
Overall	107.0	104.8	102.0	100.2	98.4	96.5	96.5	96.0	128.9

(t) Run 20.

Nozzle diameter, D_n, 5.24 cm	V-gutter reverser
Spacing ratio, x/D_n, 0.42	Reverser orientation, α, 0°
Pressure ratio (static), P_n/P_a, 1.69	Superficial velocity,[a] V_n, 209 m/sec
Nozzle inlet temperature, T_n, 293 K	Ambient temperature, T_a, 297 K
Ambient pressure, P_a, 99.1 kN/m^2 abs	Relative humidity, 45 percent

1/3-Octave-band center frequency, f_c, Hz	Angle from nozzle axis, θ, deg								Power level, PWL, dB re 10^{-13} W
	160	130	110	90	70	50	40	5	
	Sound pressure level, SPL, dB re 20 μN/m^2								
200	68.0	66.0	67.3	73.0	73.0	68.5	68.3	69.3	97.9
250	68.0	67.7	68.3	74.0	74.0	70.0	70.7	71.7	99.1
315	73.0	73.0	73.7	78.0	78.0	75.3	76.7	77.0	103.7
400	76.3	77.0	77.0	80.7	81.3	80.3	81.0	82.0	107.3
500	78.0	78.7	79.0	82.7	83.0	81.7	81.7	82.3	108.9
630	77.4	77.0	77.0	80.7	80.7	80.0	79.4	80.7	106.9
800	87.0	85.0	86.0	87.0	87.0	86.4	85.7	87.0	114.0
1000	90.0	87.0	86.0	88.7	88.7	87.7	87.4	90.0	115.7
1250	95.4	90.0	91.0	92.0	92.0	91.7	90.4	92.4	119.5
1600	92.4	91.0	92.7	94.0	94.7	93.7	92.4	95.0	120.9
2000	93.7	94.7	95.1	96.4	98.1	97.7	96.1	99.7	124.1
2500	101.4	102.1	100.1	102.1	103.7	102.7	101.1	103.4	129.7
3150	101.4	98.1	99.1	103.1	102.8	102.8	102.8	104.8	129.5
4000	99.1	99.1	101.1	102.8	103.8	102.4	101.8	103.8	129.6
5000	97.5	99.1	101.8	103.1	103.5	101.6	100.6	102.8	129.4
6300	98.5	100.2	102.2	104.2	104.8	102.8	102.8	102.8	130.5
8000	98.2	100.2	102.2	103.2	103.6	102.9	103.6	99.9	130.0
10000	96.6	98.3	100.6	103.6	103.9	100.9	101.9	97.9	129.3
12500	95.4	97.4	101.4	103.4	104.0	100.0	100.0	96.7	129.0
16000	94.1	96.5	99.5	101.8	102.1	98.8	99.1	95.5	127.4
20000	92.2	94.6	97.9	100.2	100.6	96.2	96.2	93.6	125.6
Overall	108.9	109.3	111.0	113.1	113.7	111.9	111.7	112.0	139.5

[a]Based on measured flow rate and ambient pressure and temperature.

TABLE IV. - Continued. DETAILED ACOUSTIC DATA

(u) Run 21.

Nozzle diameter, D_n, 5.24 cm	V-gutter reverser
Spacing ratio, x/D_n, 0.36	Reverser orientation, α, 0^o
Pressure ratio (static), P_n/P_a, 2.03	Superficial velocity,[a] V_n, 243 m/sec
Nozzle inlet temperature, T_n, 291 K	Ambient temperature, T_a, 297 K
Ambient pressure, P_a, 99.1 kN/m^2 abs	Relative humidity, 45 percent

1/3-Octave-band center frequency, f_c, Hz	Angle from nozzle axis, θ, deg								Power level, PWL, dB re 10^{-13} W
	160	130	110	90	70	50	40	5	
	Sound pressure level, SPL, dB re 20 μN/m^2								
200	73.7	73.0	74.0	74.3	74.7	75.0	75.3	75.7	102.0
250	74.0	74.0	75.0	75.7	75.7	76.7	77.0	77.3	103.2
315	77.0	78.0	79.0	79.3	80.0	80.3	81.0	81.7	107.1
400	81.0	81.3	82.0	83.0	84.0	84.0	84.7	84.7	110.7
500	83.0	83.0	83.7	85.0	86.0	85.0	85.0	84.7	112.2
630	81.0	81.0	82.0	83.0	84.0	85.0	84.7	84.7	110.8
800	91.0	90.0	91.7	91.7	91.4	91.0	90.7	90.7	118.7
1000	94.0	93.0	92.4	94.4	94.7	93.7	93.0	93.4	121.3
1250	97.7	95.0	96.4	97.0	97.0	96.7	95.7	96.0	124.1
1600	95.7	95.4	97.0	98.0	99.0	98.7	98.0	98.7	125.3
2000	100.1	100.1	100.4	101.4	103.1	103.7	102.7	103.7	129.5
2500	109.1	107.1	107.1	109.7	110.7	110.1	109.7	109.1	136.8
3150	106.1	104.1	106.1	108.8	109.8	109.8	108.1	108.1	135.5
4000	103.1	103.1	105.1	107.1	108.4	108.1	107.1	107.1	134.2
5000	103.1	104.5	106.1	108.1	109.8	108.1	106.1	106.1	134.8
6300	104.0	105.5	107.2	109.2	110.5	107.8	107.2	106.2	135.6
8000	102.6	104.2	106.2	107.2	108.2	107.6	107.9	104.2	134.3
10000	101.6	102.6	105.3	108.3	108.3	106.3	106.3	102.3	133.9
12500	101.0	102.4	106.0	107.4	108.0	105.4	104.4	100.4	133.3
16000	99.8	101.5	104.5	106.5	107.1	104.5	103.8	99.5	132.3
20000	98.6	99.6	103.2	104.6	105.9	102.6	101.9	97.6	130.8
Overall	114.4	114.3	116.1	118.1	119.1	117.8	117.1	115.9	144.7

[a]Based on measured flow rate and ambient pressure and temperature.

(v) Run 22.

Nozzle diameter, D_n, 5.24 cm	V-gutter reverser
Spacing ratio, x/D_n, 0.27	Reverser orientation, α, 0^o
Pressure ratio (static), P_n/P_a, 2.47	Superficial velocity,[a] V_n, 312 m/sec
Nozzle inlet temperature, T_n, 291 K	Ambient temperature, T_a, 297 K
Ambient pressure, P_a, 99.1 kN/m^2 abs	Relative humidity, 45 percent

1/3-Octave-band center frequency, f_c, Hz	Angle from nozzle axis, θ, deg								Power level, PWL, dB re 10^{-13} W
	160	130	110	90	70	50	40	5	
	Sound pressure level, SPL, dB re 20 μN/m^2								
200	75.3	75.0	75.3	75.5	77.7	77.3	78.0	79.0	104.1
250	75.0	75.0	76.0	77.7	78.3	79.0	80.0	81.0	105.4
315	79.0	79.0	80.0	81.3	82.0	83.0	84.0	85.0	109.3
400	83.0	83.0	83.0	84.0	85.3	86.3	87.0	88.0	112.5
500	85.0	85.0	84.7	85.0	86.0	87.0	87.7	87.0	113.4
630	83.7	84.0	84.0	85.0	85.7	87.0	88.0	88.0	113.2
800	92.0	90.0	91.0	91.0	92.0	92.7	92.7	93.4	119.3
1000	95.0	92.0	93.0	96.0	97.0	97.0	97.0	97.0	123.2
1250	101.0	96.0	97.0	97.0	98.0	98.0	98.0	97.0	125.4
1600	96.7	96.0	97.7	98.0	99.7	100.7	100.0	100.0	126.3
2000	98.1	99.1	100.1	100.4	102.1	104.1	103.1	103.7	129.0
2500	99.0	101.1	101.1	103.1	105.1	105.1	104.1	105.1	130.8
3150	102.1	102.1	103.1	106.1	108.1	108.4	107.1	106.8	133.6
4000	106.1	106.1	108.1	111.1	114.1	113.1	111.8	112.1	138.7
5000	105.1	106.1	108.5	111.1	113.1	111.8	109.8	108.5	137.5
6300	104.8	106.2	108.5	109.2	113.2	111.2	111.2	107.8	137.6
8000	104.2	105.9	108.9	109.9	111.2	110.2	109.9	106.9	136.8
10000	104.3	105.3	109.3	111.3	111.9	110.3	110.3	105.9	137.4
12500	103.4	105.4	109.4	110.4	112.9	109.4	108.4	105.4	136.9
16000	102.8	104.5	108.5	109.5	111.5	107.8	107.5	103.8	136.0
20000	102.6	103.6	107.6	108.6	110.6	106.6	105.6	102.2	135.0
Overall	114.3	115.2	118.1	119.7	121.8	120.2	119.4	117.7	146.7

[a]Based on measured flow rate and ambient pressure and temperature.

TABLE IV. - Concluded. DETAILED ACOUSTIC DATA

(w) Run 23.

Nozzle diameter, D_n, 5.24 cm	V-gutter reverser
Spacing ratio, x/D_n, 0.18	Reverser orientation, α, 0^o
Pressure ratio (static), P_n/P_a, 1.59	Superficial velocity,[a] V_n, 239 m/sec
Nozzle inlet temperature, T_n, 292 K	Ambient temperature, T_a, 297 K
Ambient pressure, P_a, 99.1 kN/m^2 abs	Relative humidity, 45 percent

1/3-Octave-band center frequency, f_c, Hz	Angle from nozzle axis, θ, deg								Power level, PWL, dB re 10^{-13} W
	160	130	110	90	70	50	40	5	
	Sound pressure level, SPL, dB re 20 μN/m^2								
200	65.5	69.5	67.5	67.0	70.5	66.5	67.7	68.3	95.9
250	65.0	68.5	67.5	67.5	69.3	68.0	69.0	70.0	95.8
315	68.0	70.0	70.0	70.7	72.0	72.7	72.7	73.0	98.8
400	71.0	72.5	73.3	74.0	74.7	75.3	76.0	76.3	101.8
500	74.3	75.0	74.7	76.0	77.0	77.0	77.0	78.0	103.7
630	75.0	75.4	74.7	74.4	75.4	77.4	77.0	79.0	103.4
800	78.4	78.4	78.7	79.0	80.4	82.4	82.7	83.4	107.9
1000	80.4	80.4	80.0	81.0	82.7	84.0	83.7	84.4	109.6
1250	86.0	85.4	84.0	85.0	87.7	89.4	89.0	88.4	114.5
1600	86.0	87.0	87.0	87.0	89.0	91.0	90.7	92.0	116.3
2000	88.7	89.1	89.1	90.1	93.1	94.1	92.1	94.1	119.0
2500	89.7	89.4	90.1	92.1	95.1	95.1	94.1	95.7	120.5
3150	90.8	90.1	90.8	94.1	97.8	96.1	94.1	97.4	122.1
4000	91.8	91.4	92.1	96.1	100.8	97.1	95.1	98.8	124.1
5000	90.8	92.5	93.8	95.1	102.1	98.1	95.8	98.8	124.9
6300	90.8	93.2	95.2	97.2	104.2	97.2	95.8	98.8	126.3
8000	90.2	93.2	95.6	97.2	103.9	96.2	94.2	98.9	126.0
10000	89.6	92.6	95.6	97.3	102.3	94.3	93.9	97.3	124.9
12500	88.7	91.7	95.7	97.4	100.4	93.0	92.7	96.0	123.8
16000	88.8	91.5	95.1	97.1	98.5	92.1	92.5	94.1	122.8
20000	87.9	89.9	93.6	95.6	96.6	90.2	89.6	91.2	121.1
Overall	100.8	102.3	104.5	106.4	111.2	106.1	104.8	107.7	134.3

[a]Based on measured flow rate and ambient pressure and temperature.

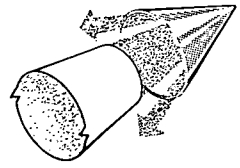

(a) Conical V-umbrella (ref. 13).

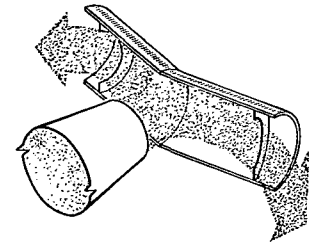

(b) Clamshell (ref. 13).

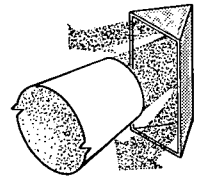

(c) Longitudinal V-gutter (ref. 13).

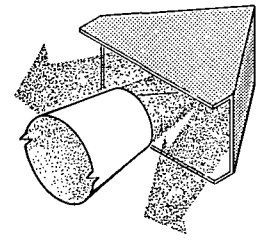

(d) V-gutter and cover plates - current test configuration (ref. 13).

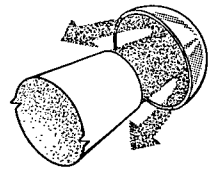

(e) Hemisphere (refs. 3 and 13).

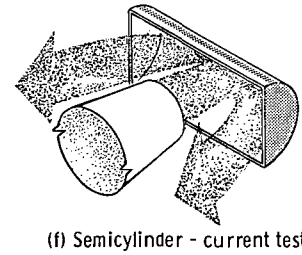

(f) Semicylinder - current test configuration (ref. 3).

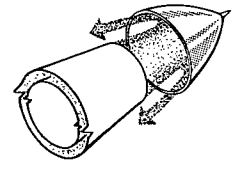

(g) Annular target (ref. 12).

Figure 1. - Target-type thrust reverser configurations.

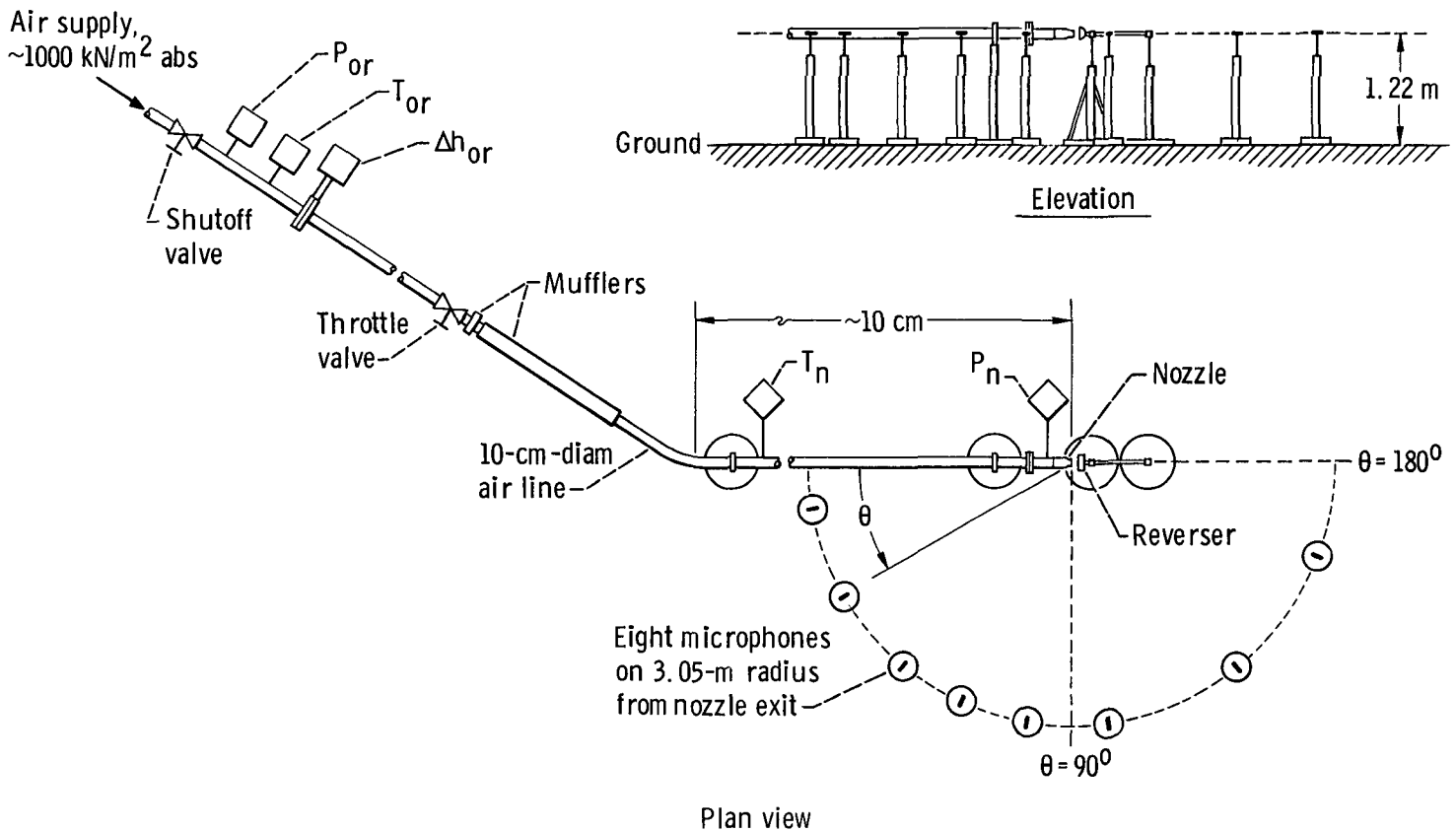

Figure 2. - Schematic diagram of acoustic apparatus.

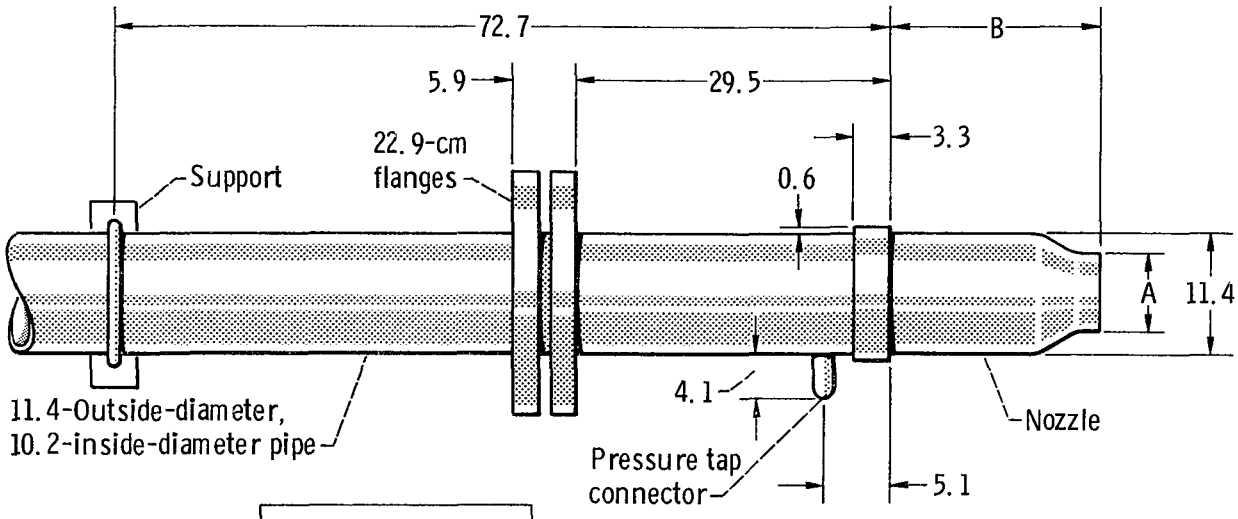

Nozzle dimensions		
Inside diameter, D_n	A	B
5.24	6.0	19.0
7.78	8.9	20.0

Figure 3. - Detailed sketch (top view) of air supply system near nozzle. (All dimensions are in centimeters.)

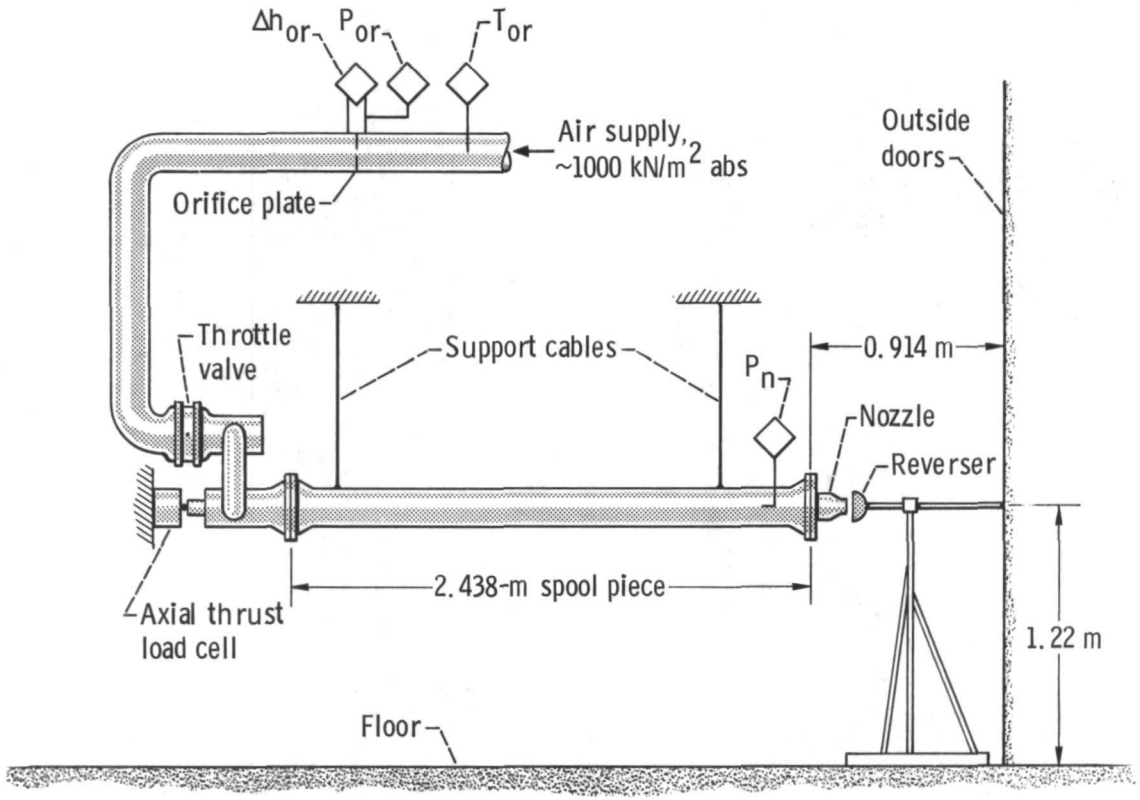

Figure 4. - Schematic diagram of auxiliary flow apparatus.

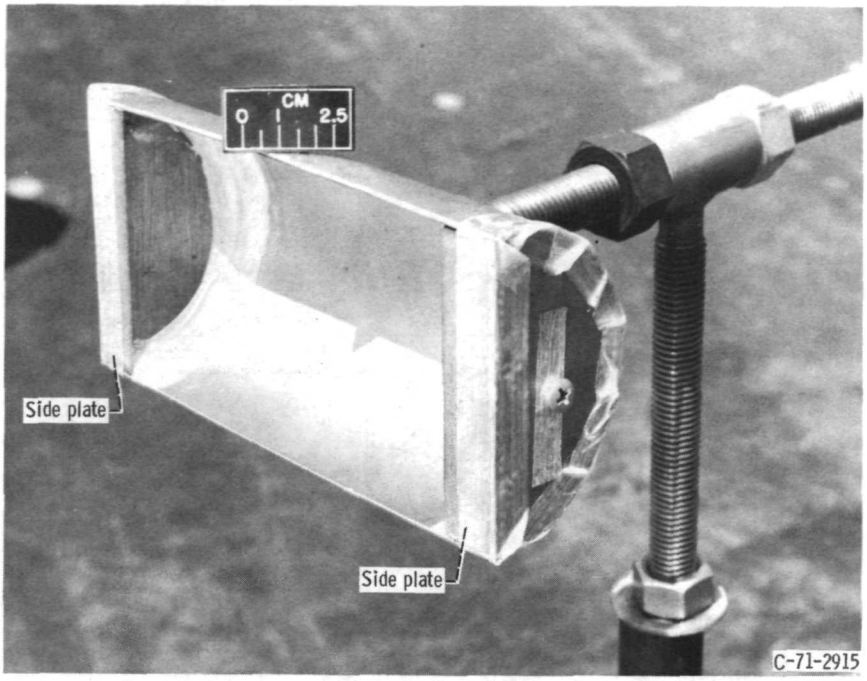

(a) Smaller.

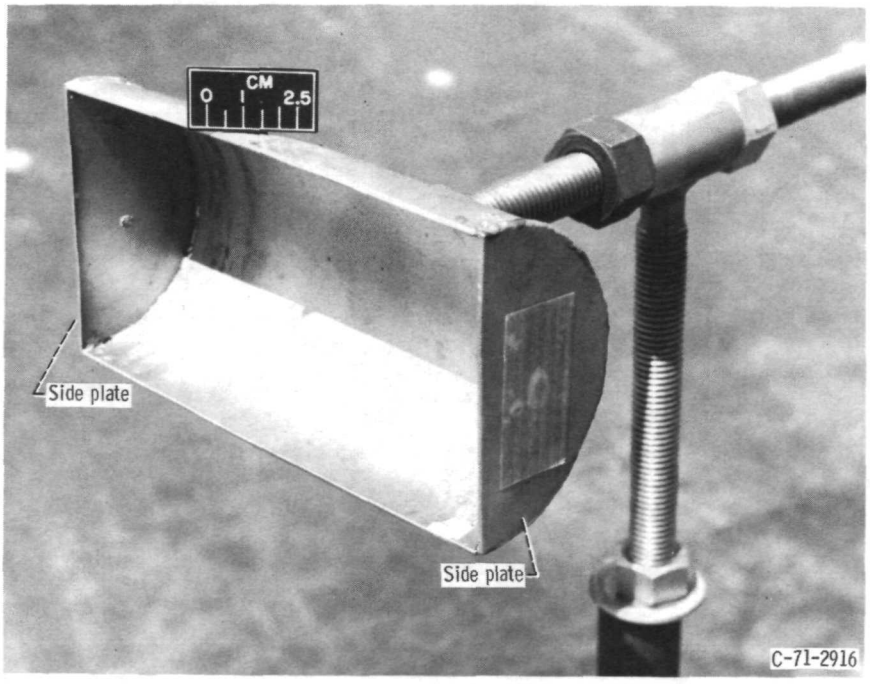

(b) Larger.

Figure 5. - Semicylindrical thrust reversers.

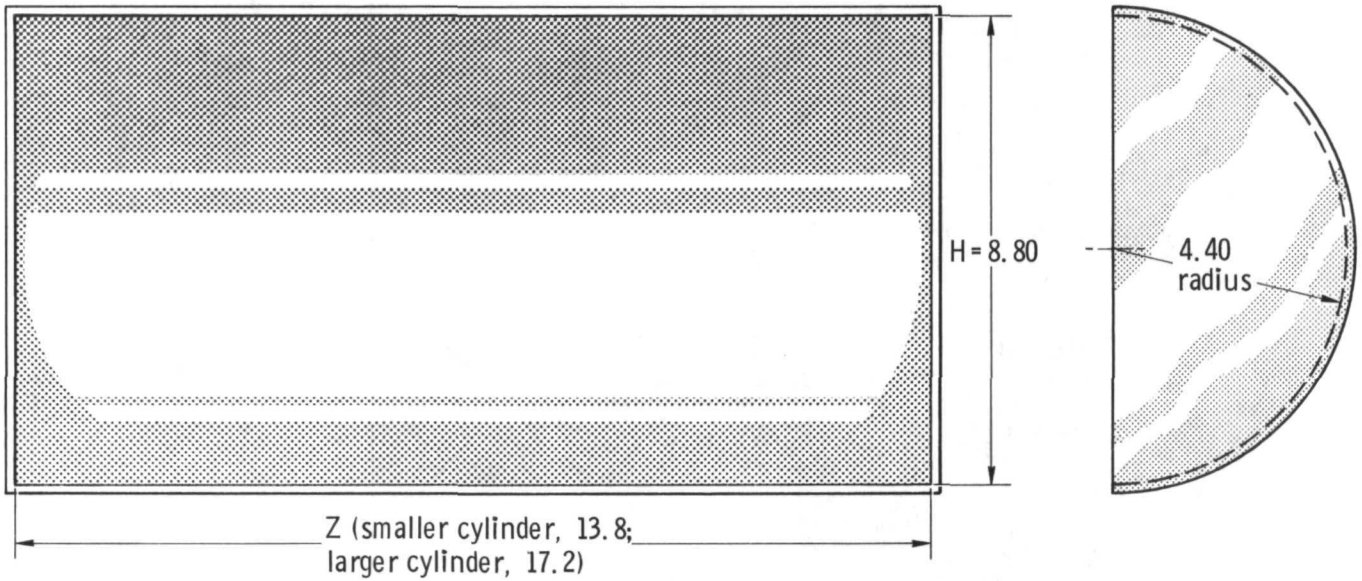

(c) Sketch of semicylindrical thrust reversers. (All dimensions are in centimeters.)

Figure 5. - Concluded.

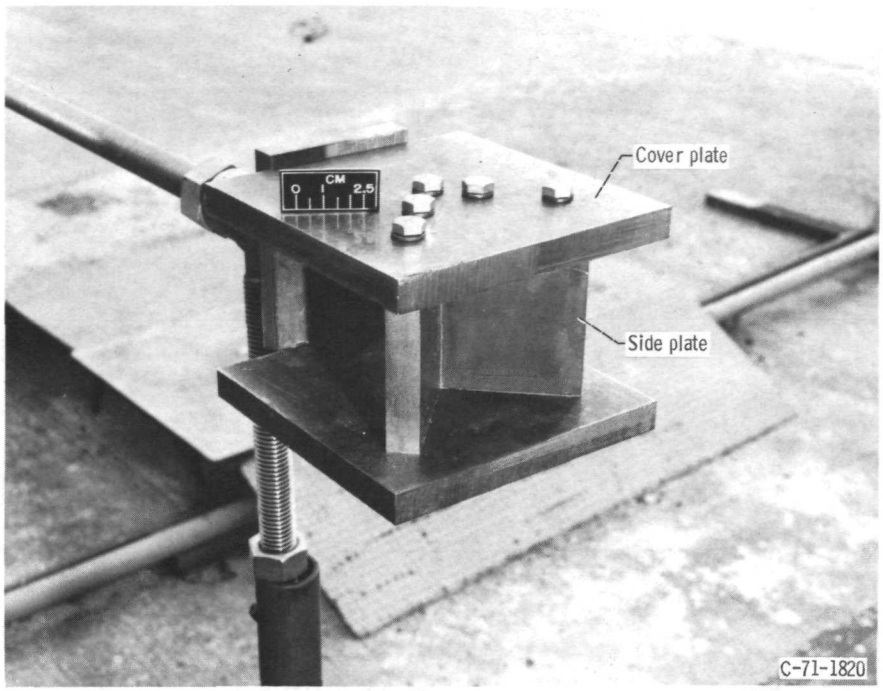

(a) Reverser with cover plates.

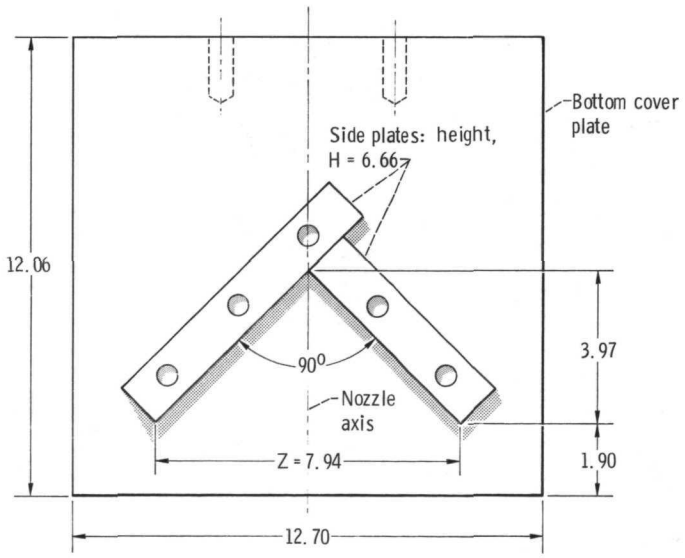

(b) Top view of V-gutter thrust reverser with top cover plate removed. (All dimensions are in centimeters.)

Figure 6. - V-gutter thrust reverser.

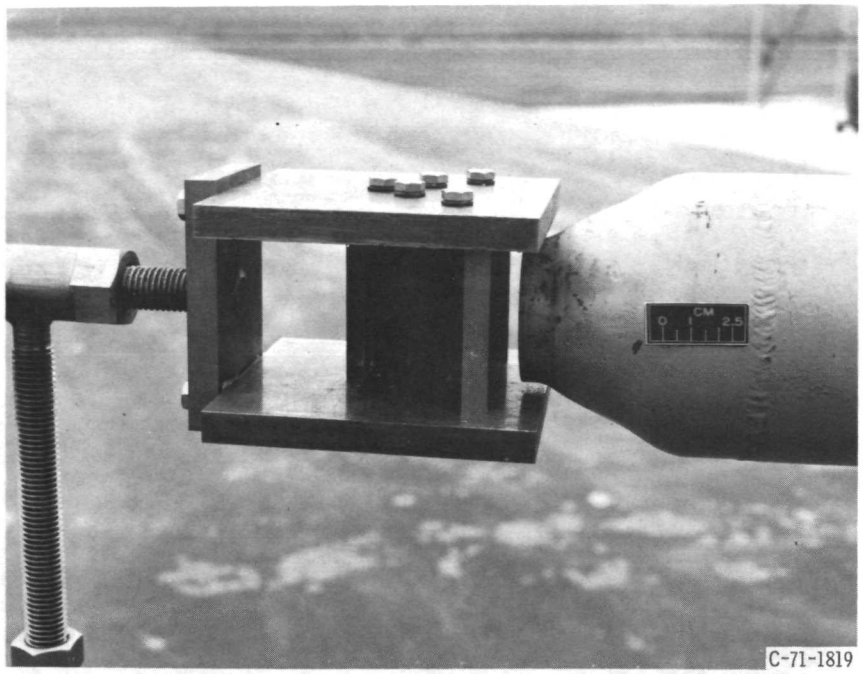

(a) V-gutter reverser at horizontal position ($\alpha = 0°$).

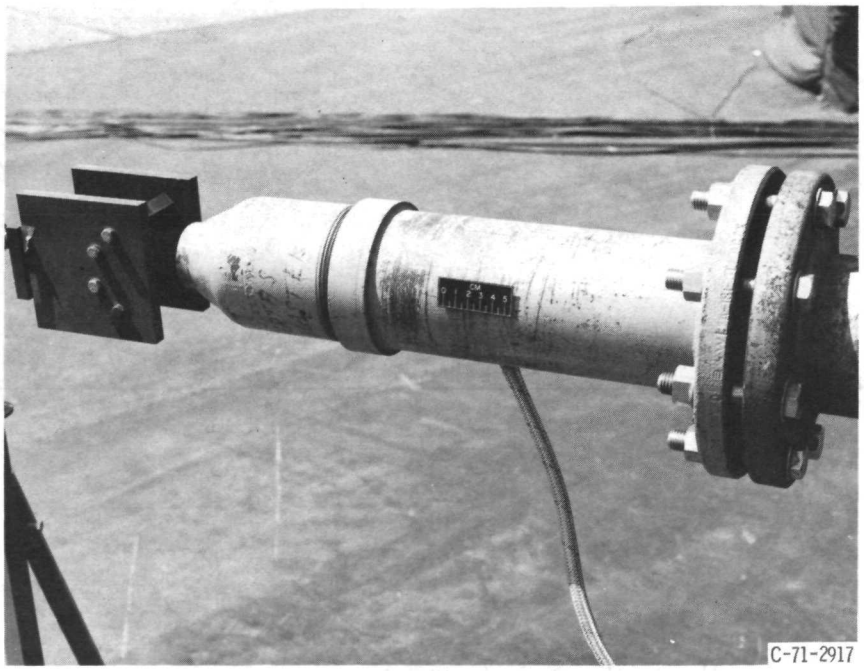

(b) V-gutter reverser at vertical position ($\alpha = 90°$).

Figure 7. - Thrust reversers mounted at 5.24-centimeter-diameter nozzle exit.

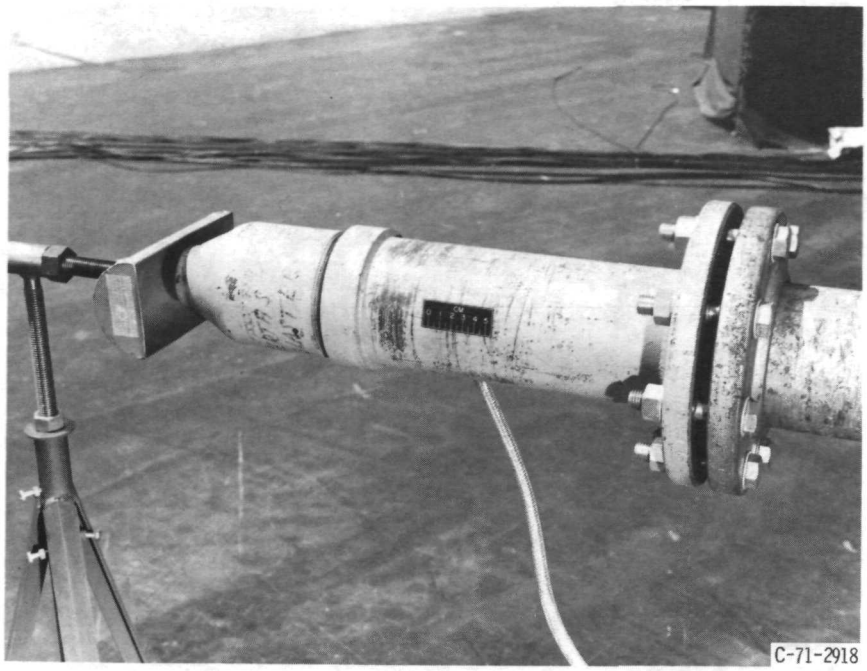

(c) Larger semicylindrical reverser at horizontal position ($\alpha = 0°$).

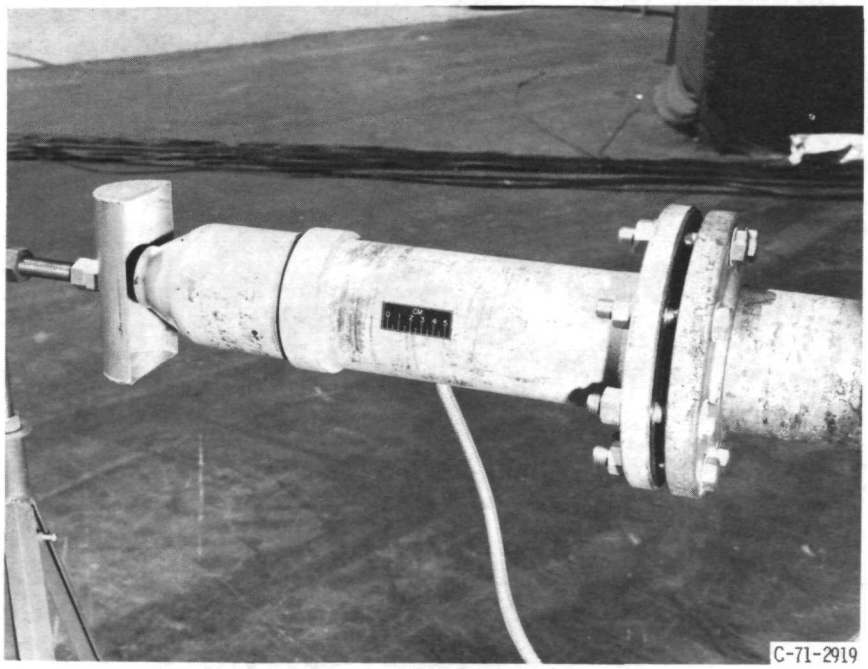

(d) Larger semicylindrical reverser at vertical position ($\alpha = 90°$).

Figure 7. - Concluded.

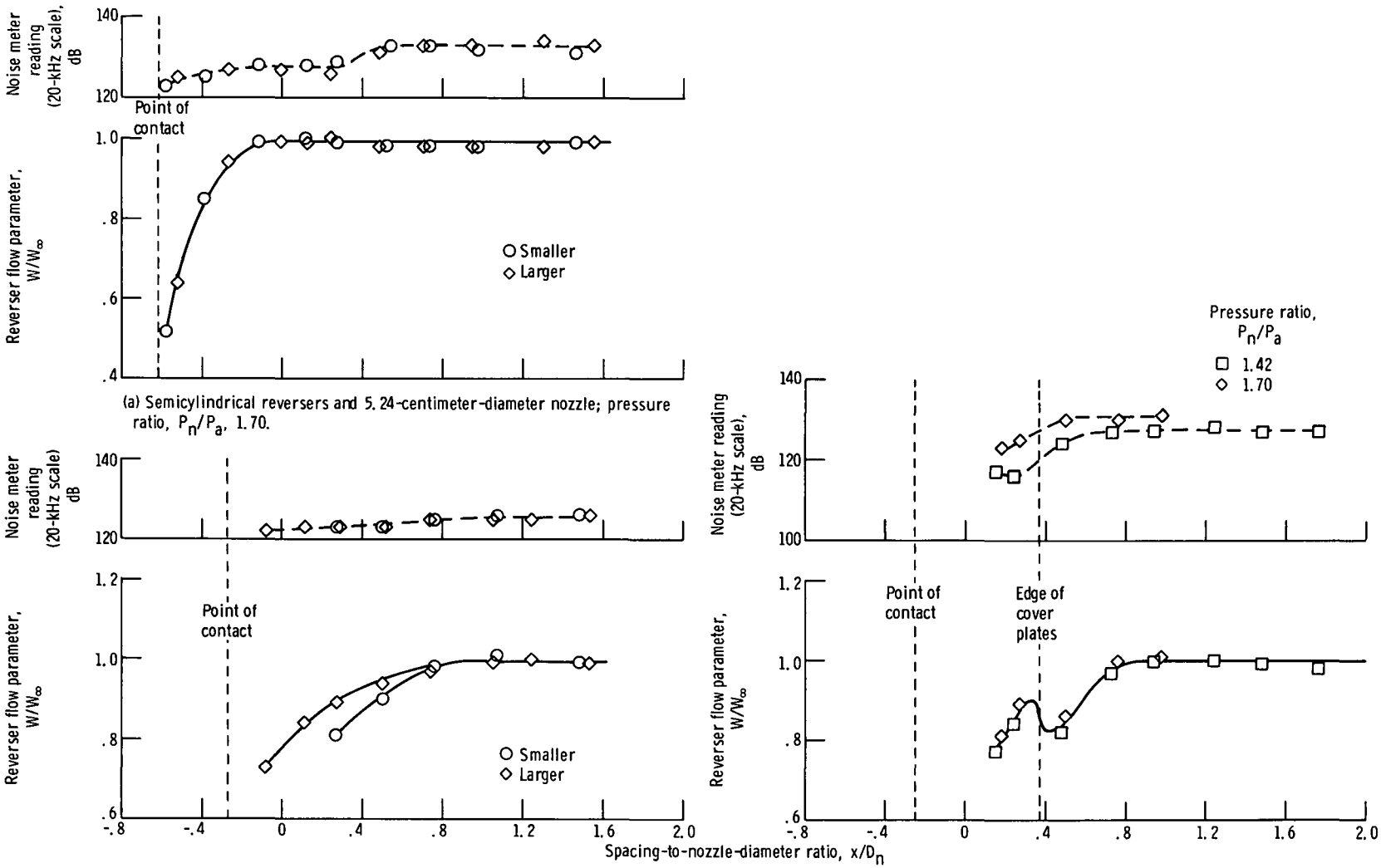

(a) Semicylindrical reversers and 5.24-centimeter-diameter nozzle; pressure ratio, P_n/P_a, 1.70.

(b) Semicylindrical reversers and 7.78-centimeter-diameter nozzle; pressure ratio, P_n/P_a, 1.40.

(c) V-gutter reverser and 5.24-centimeter-diameter nozzle.

Figure 8. - Effects of reverser spacing on flow and noise indications.

	Reverser	Nozzle diameter, D_n, cm	Pressure ratio, P_n/P_a	Spacing ratio, x/D_n	Reverser orientation, α, deg
▷	None	5.24	1.72	--	--
◁	Smaller semi-cylindrical	5.24	1.72	0	0

Tailed symbol denotes microphone in jet

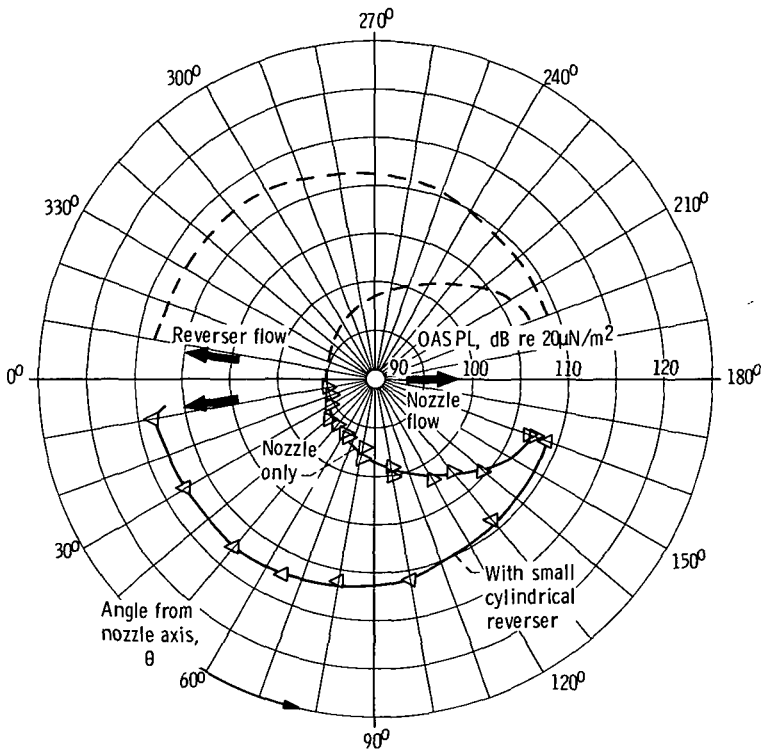

Figure 9. - Effect of thrust reversal on noise directivity patterns. Comparison of smaller cylindrical reverser and 5.24-centimeter-diameter nozzle with bare nozzle only; overall sound pressure level at 3.05-meter radius.

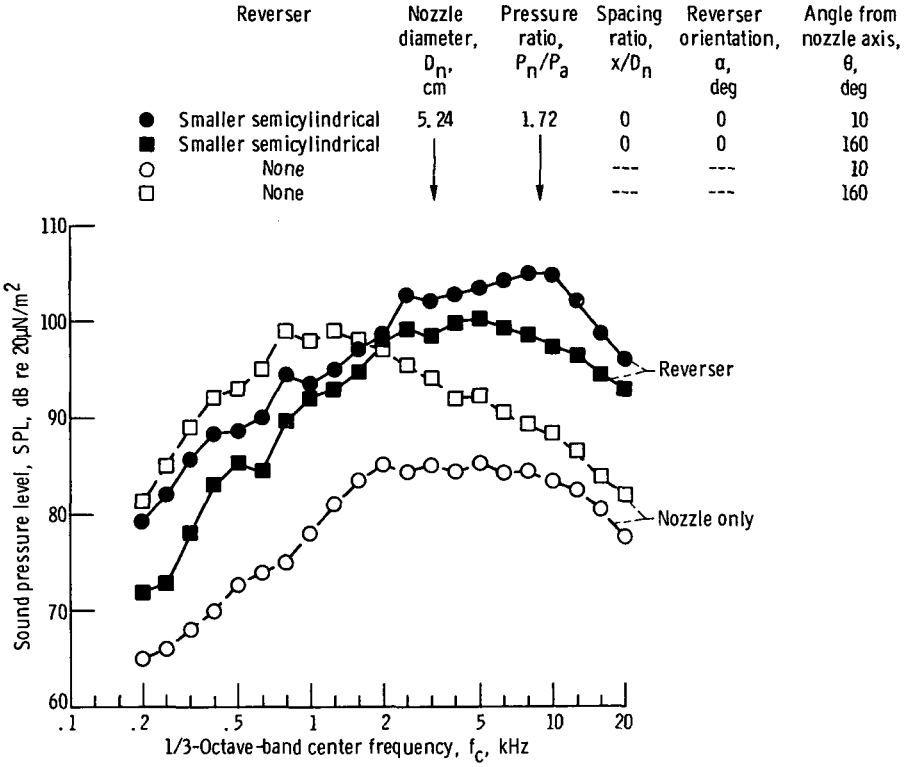

Figure 10. - Effect of thrust reversal on noise spectrum. Comparison of smaller semicylindrical reverser and 5.24-centimeter-diameter nozzle with bare nozzle only at two angular positions. Pressure ratio, P_n/P_a, 1.72.

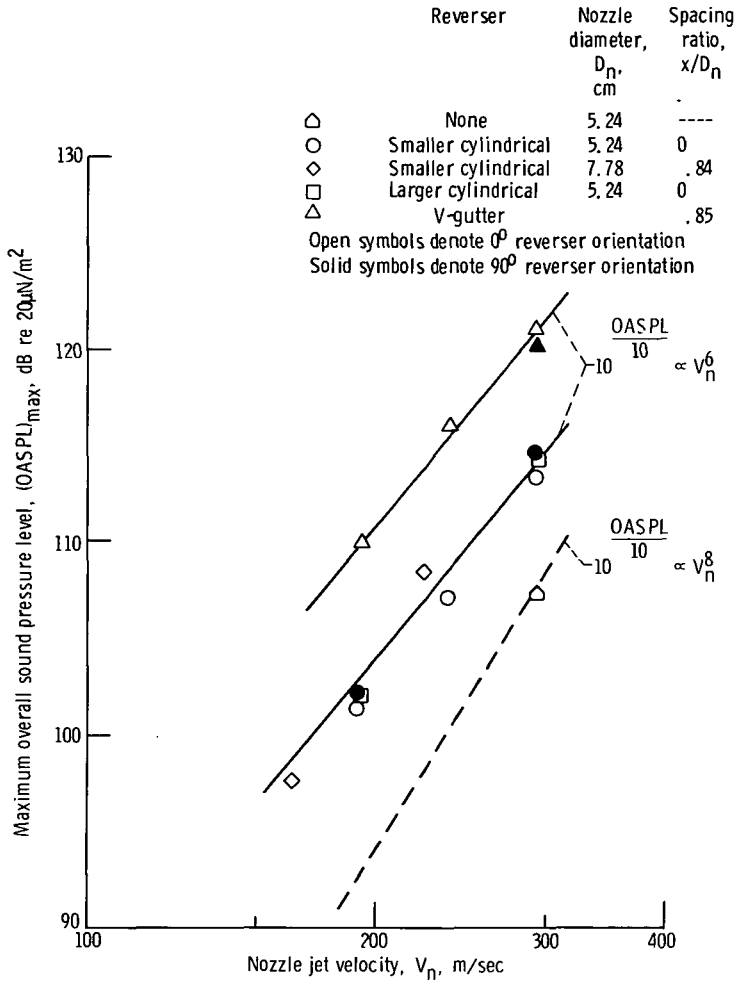

Figure 11. - Effect of nozzle jet velocity on maximum overall sound pressure level at optimum reverser spacings.

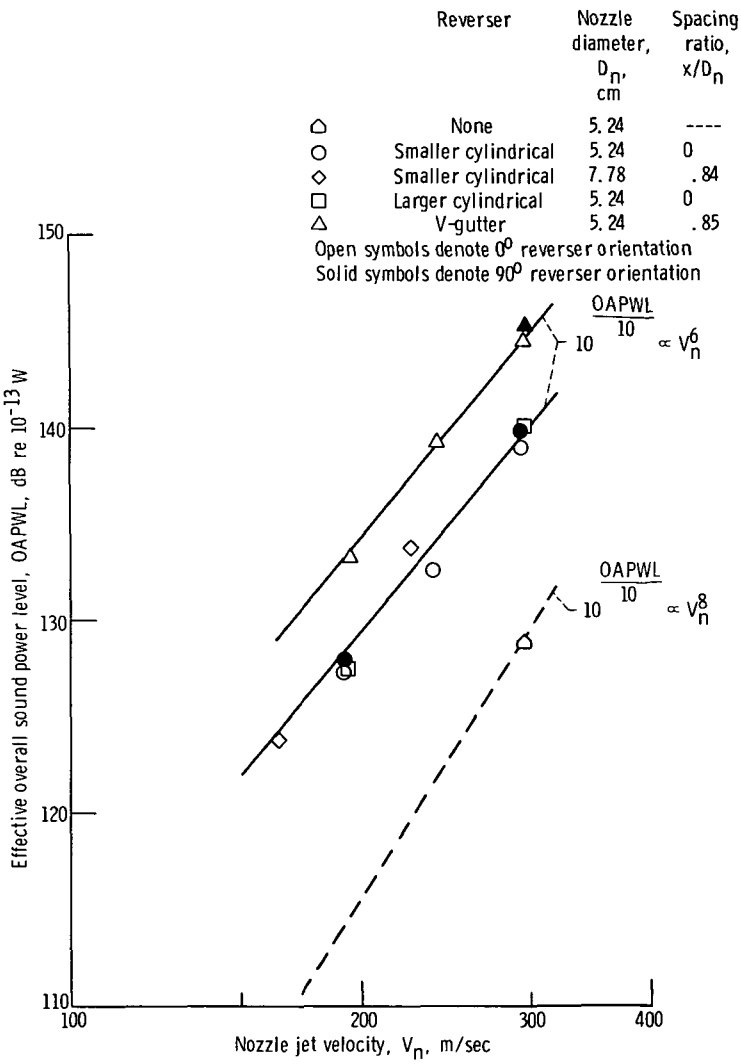

Figure 12. - Effect of nozzle jet velocity on overall sound power level at optimum reverser spacings.

	Reverser	Nozzle diameter, D_n, cm	Area ratio, A_f/A_n	Pressure ratio, P_n/P_a	Spacing ratio, x/D_n	Reverser orientation, α, deg
◇	Smaller semi-cylindrical	5.24	5.63	1.25	0 (opt.)	0
□				1.42		
○				1.72		

Tailed symbols denote data taken with microphone in jet

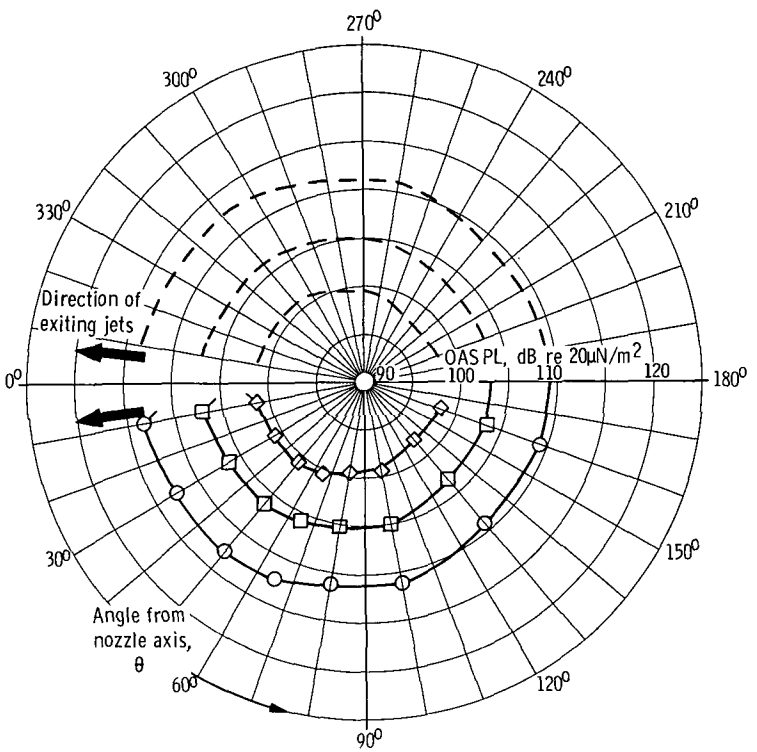

(a) Smaller semicylindrical reverser and 5.24-centimeter-diameter nozzle.

	Reverser	Nozzle diameter, D_n cm	Area ratio, A_f/A_n	Pressure ratio, P_n/P_a	Spacing ratio, x/D_n	Reverser orientation, α, deg
□	Smaller semi-cylindrical	7.78	2.55	1.17	0.84 (opt.)	0
○				1.36		

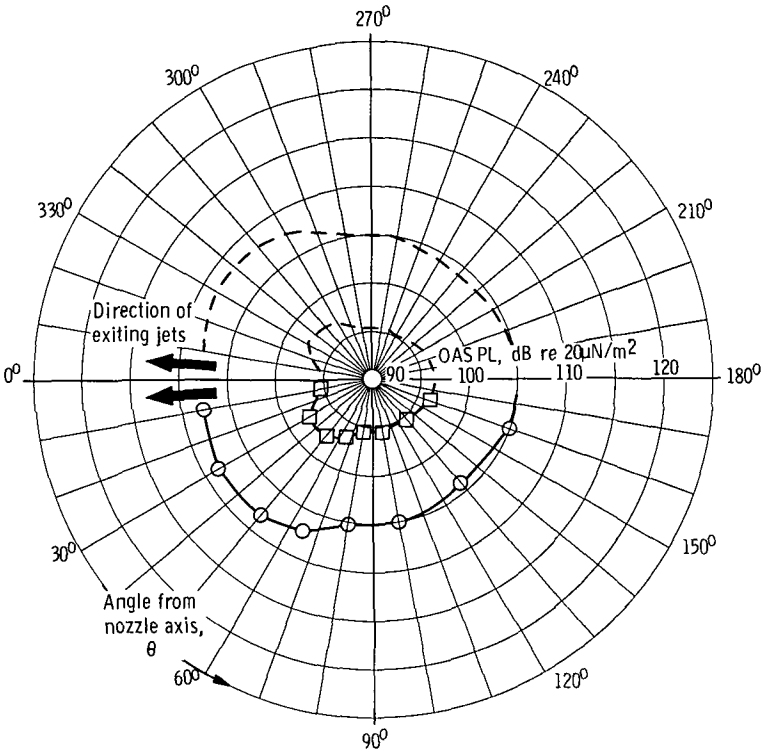

(b) Smaller semicylindrical reverser and 7.78-centimeter-diameter nozzle.

Figure 13. - Effect of pressure ratio on overall sound pressure level (OASPL) directivity patterns at 3.05-meter radius. Reverser at optimum spacing.

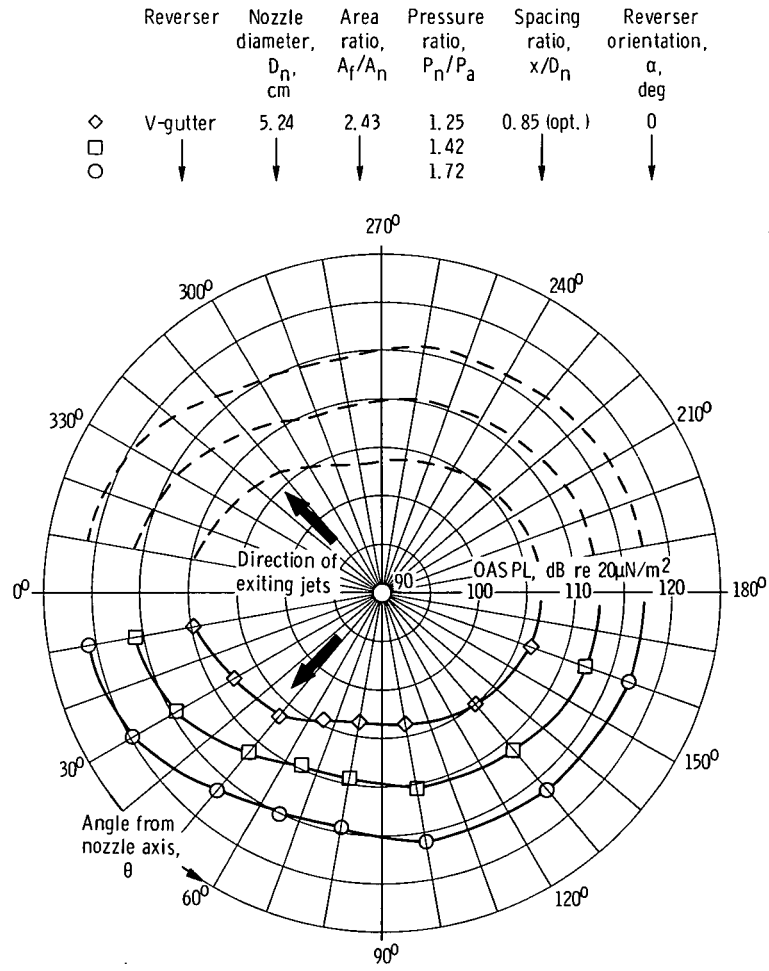

(c) V-gutter reverser and 5.24-centimeter-diameter nozzle.

Figure 13. - Concluded.

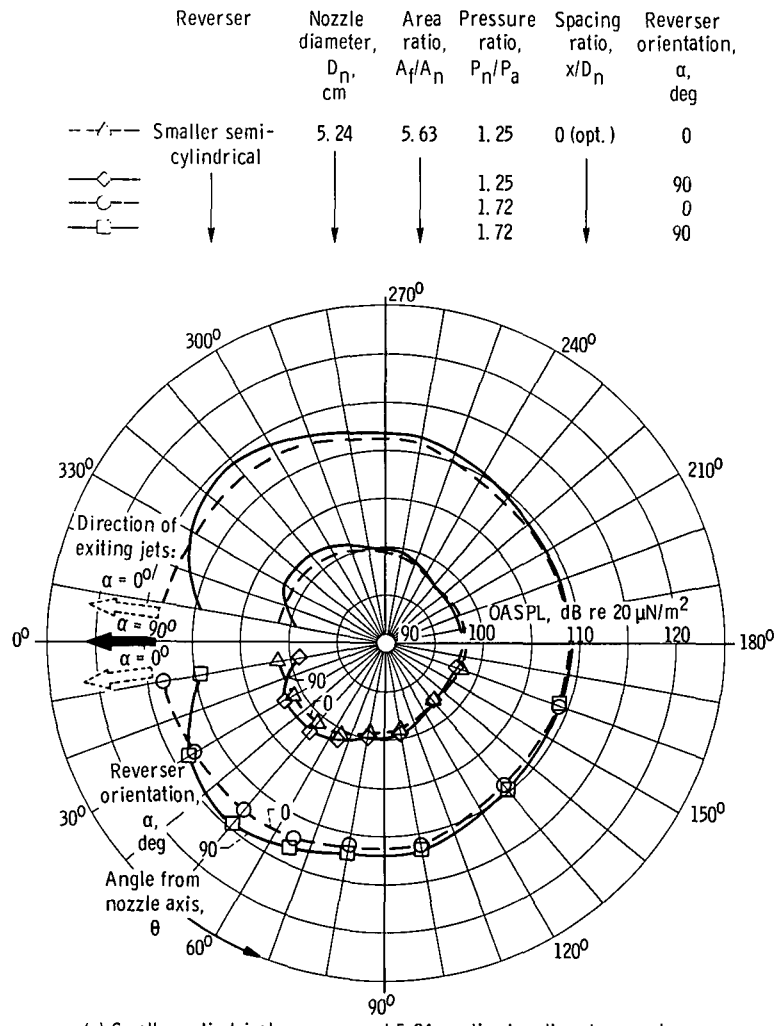

(a) Smaller cylindrical reverser and 5.24-centimeter-diameter nozzle.

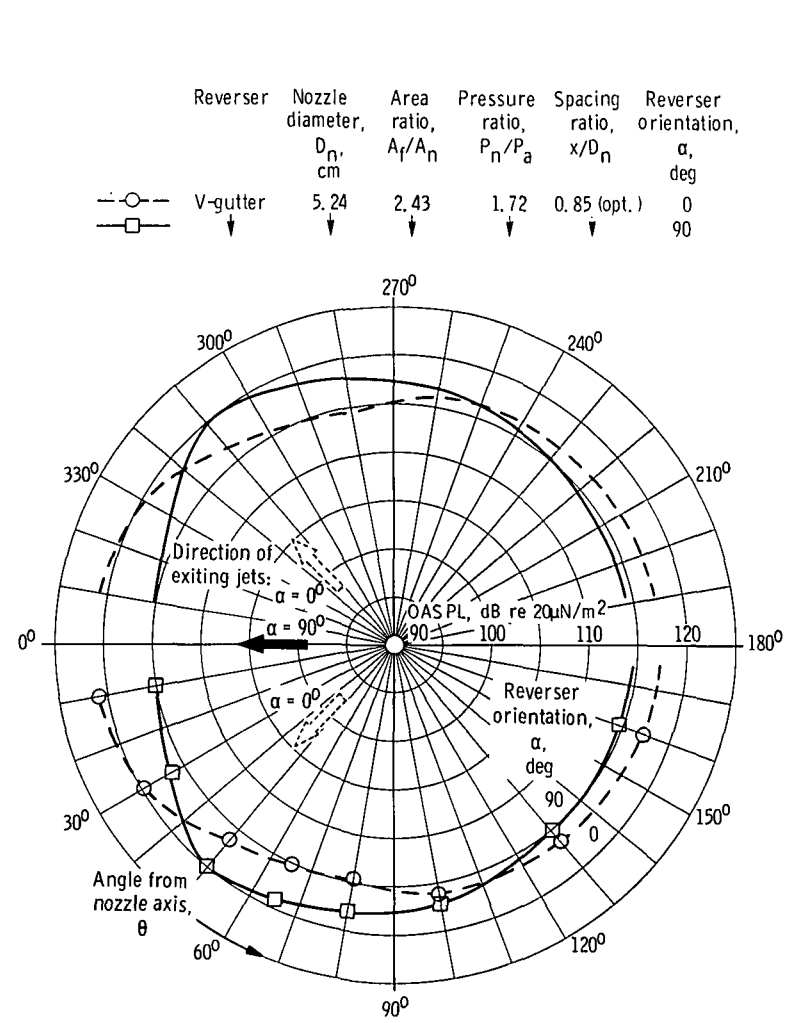

(b) V-gutter reverser and 5.24-centimeter-diameter nozzle.

Figure 14. - Effect of reverser orientation on overall sound pressure level (OASPL) directivity patterns at 3.05-meter radius. Reverser at optimum spacing.

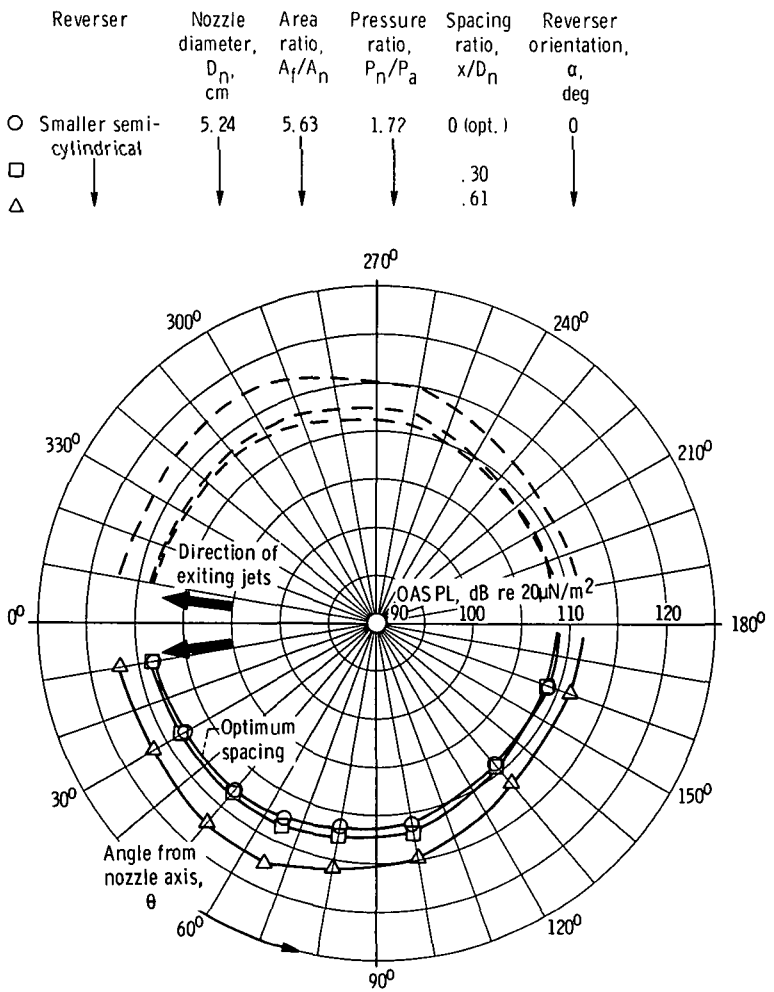

(a) Smaller cylindrical reverser and 5.24-centimeter-diameter nozzle.

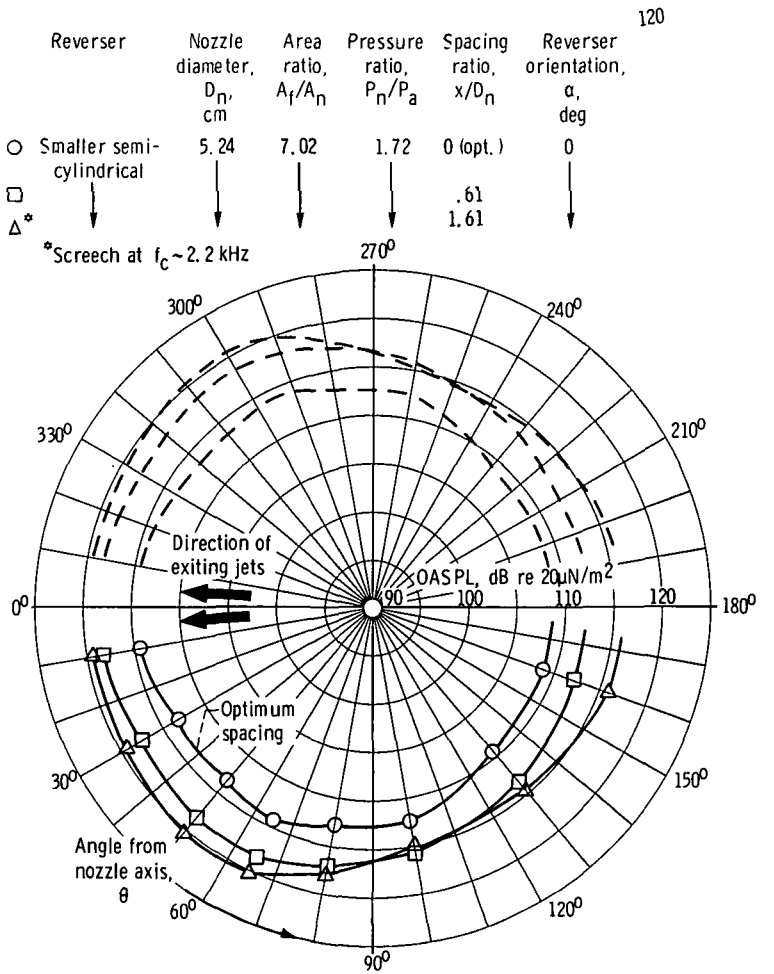

(b) Larger cylindrical reverser with 5.24-centimeter-diameter nozzle.

Figure 15. - Effect of reverser spacing on overall sound pressure level (OASPL) directivity patterns at 3.05-meter radius.

	Reverser	Nozzle diameter, D_n, cm	Area ratio, A_f/A_n	Pressure ratio, P_n/P_a	Spacing ratio, x/D_n	Reverser orientation, α, deg	Weight flow ratio, W/W_∞
○	V-gutter	5.24	2.43	1.72	0.85 (opt.)	0	1.00
□				1.72*	.42		.64
△				1.59*	.18		.73

*Nozzle throat static pressure greater than atmospheric

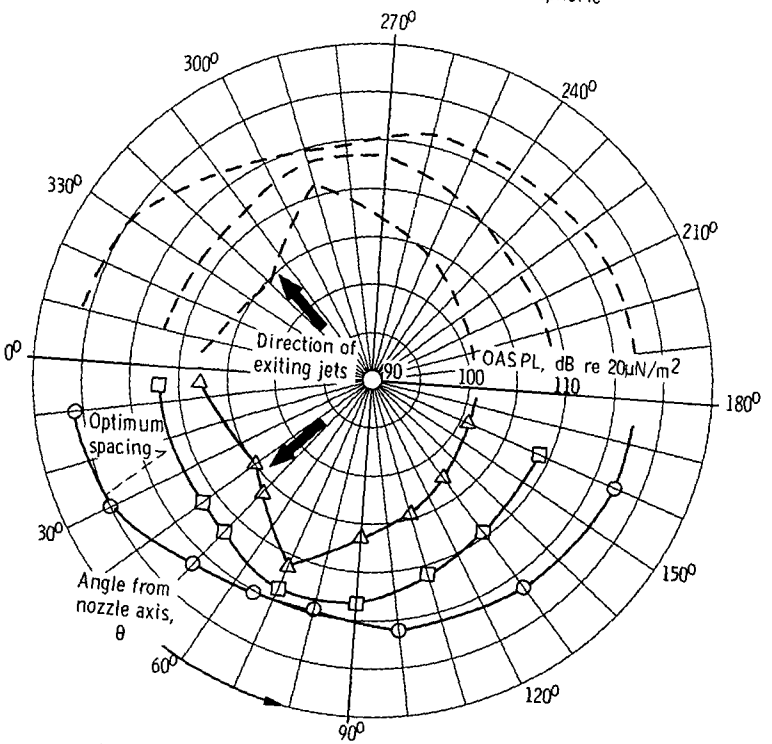

(c) V-gutter reverser and 5.24-centimeter-diameter nozzle.

Figure 15. - Concluded.

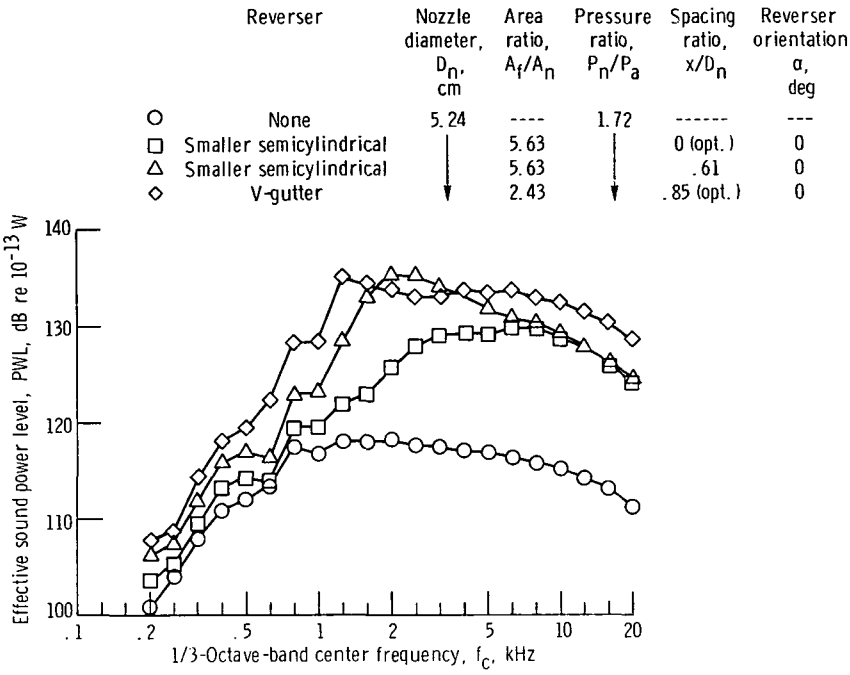

Figure 16. - Comparison of effective sound power level spectra for different types of target thrust reversers.

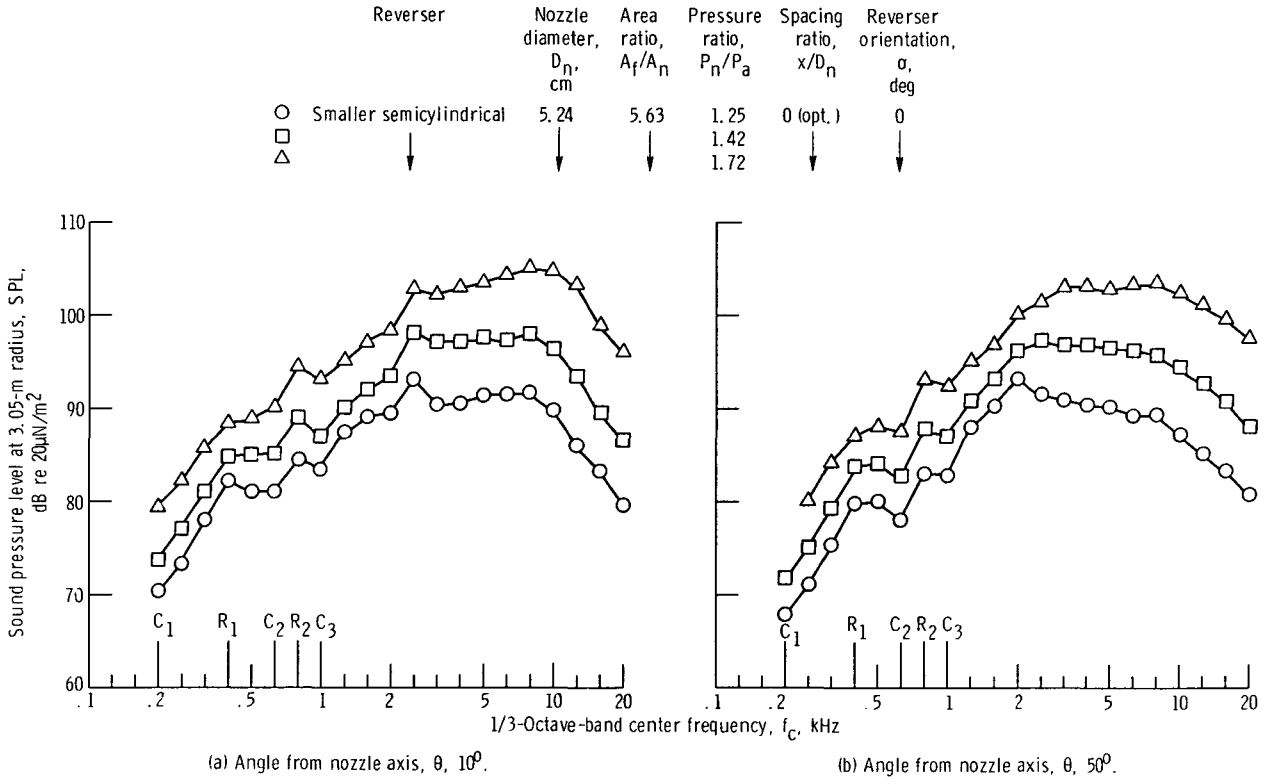

(a) Angle from nozzle axis, θ, 10^0.

(b) Angle from nozzle axis, θ, 50^0.

Figure 17. - Effect of pressure ratio on sound pressure level spectrum at different angular positions with small cylindrical reverser and 5.24-centimeter-diameter nozzle.

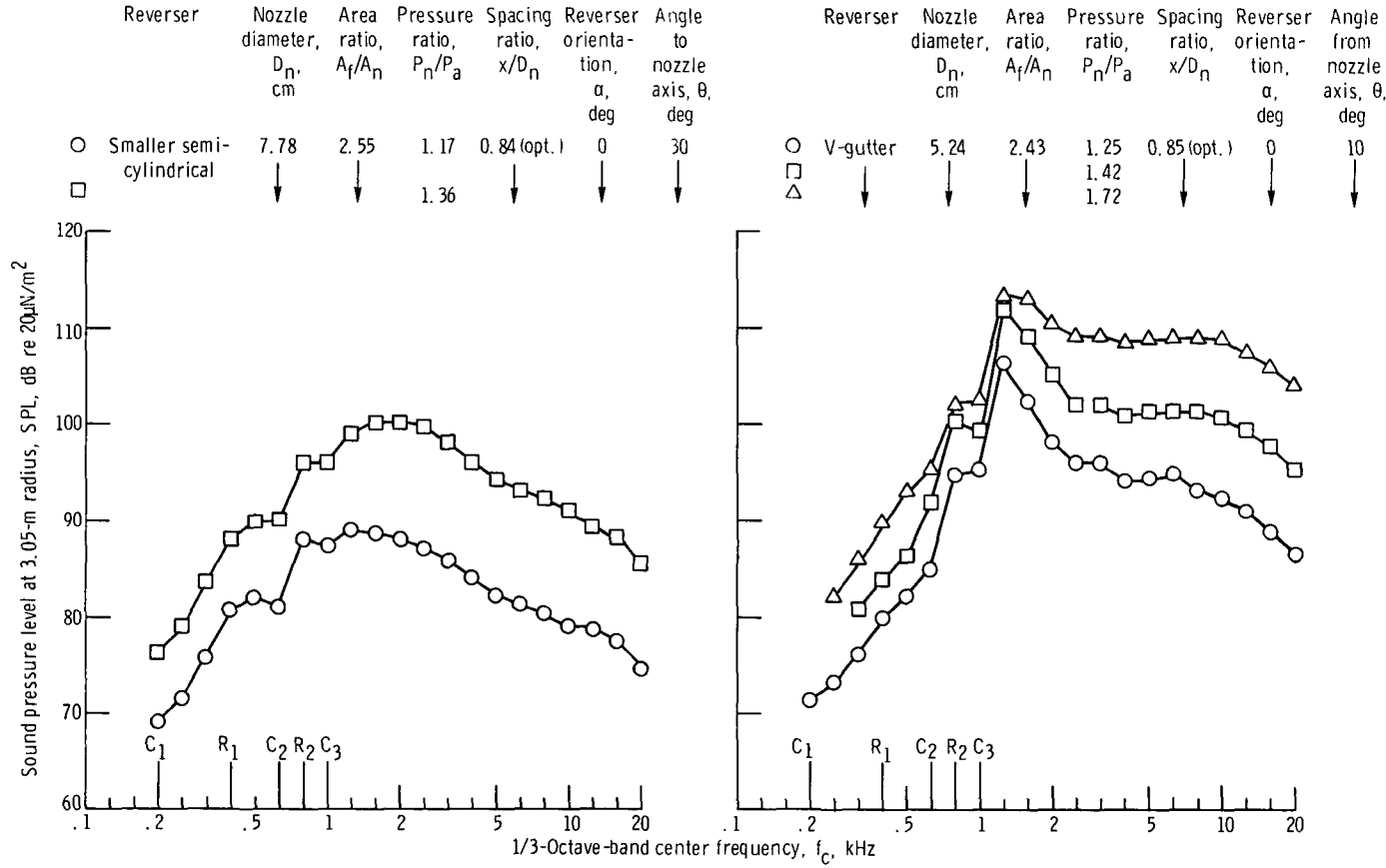

(a) Smaller semicylindrical reverser and 7.78-centimeter-diameter nozzle.

(b) V-gutter reverser and 5.24-centimeter-diameter nozzle.

Figure 18. - Effect of pressure ratio on sound pressure level spectrum in direction of maximum overall sound pressure level.

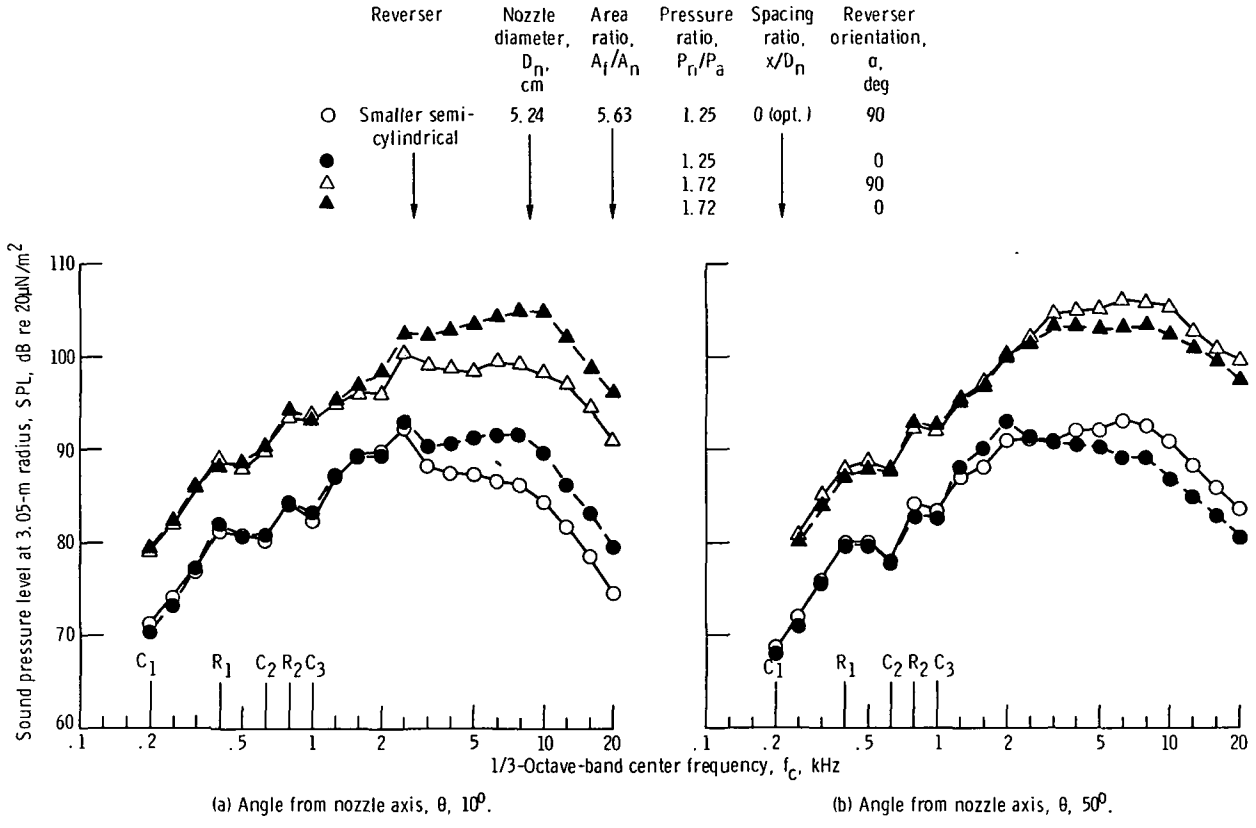

(a) Angle from nozzle axis, θ, 10°.

(b) Angle from nozzle axis, θ, 50°.

Figure 19. - Effect of reverser orientation on sound pressure level spectrum for small cylindrical reverser and 5.24-centimeter-diameter nozzle.

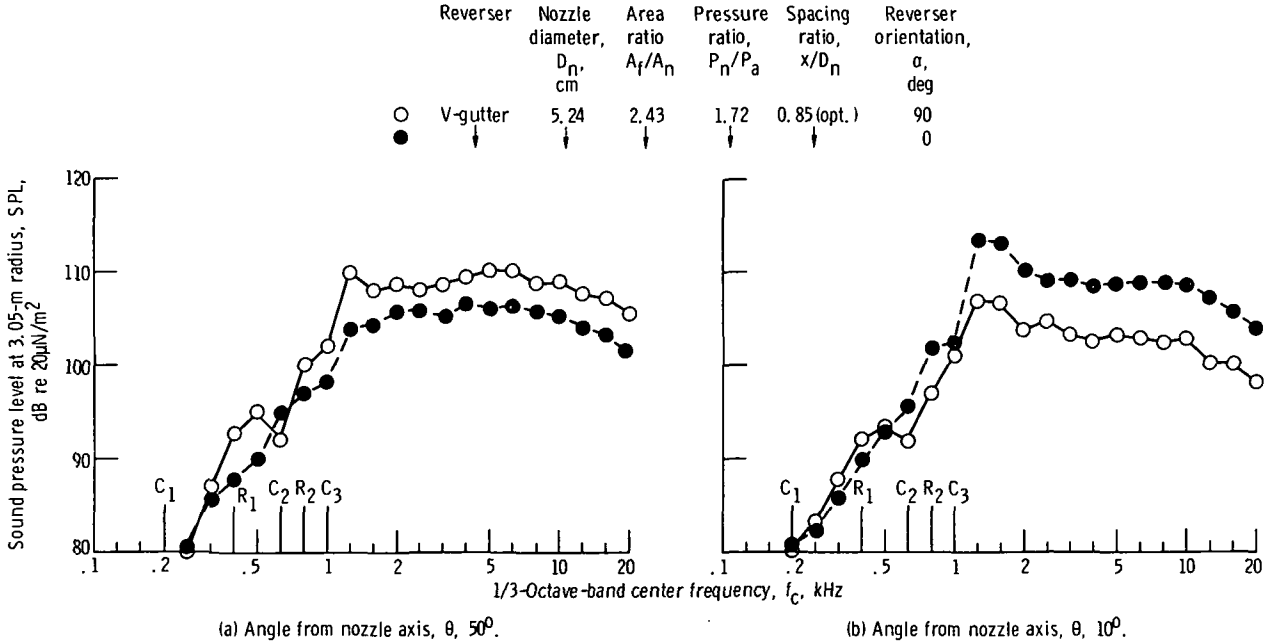

(a) Angle from nozzle axis, θ, 50°.

(b) Angle from nozzle axis, θ, 10°.

Figure 20. - Effect of reverser orientation on sound pressure level for V-gutter reverser and 5.24-centimeter-diameter nozzle.

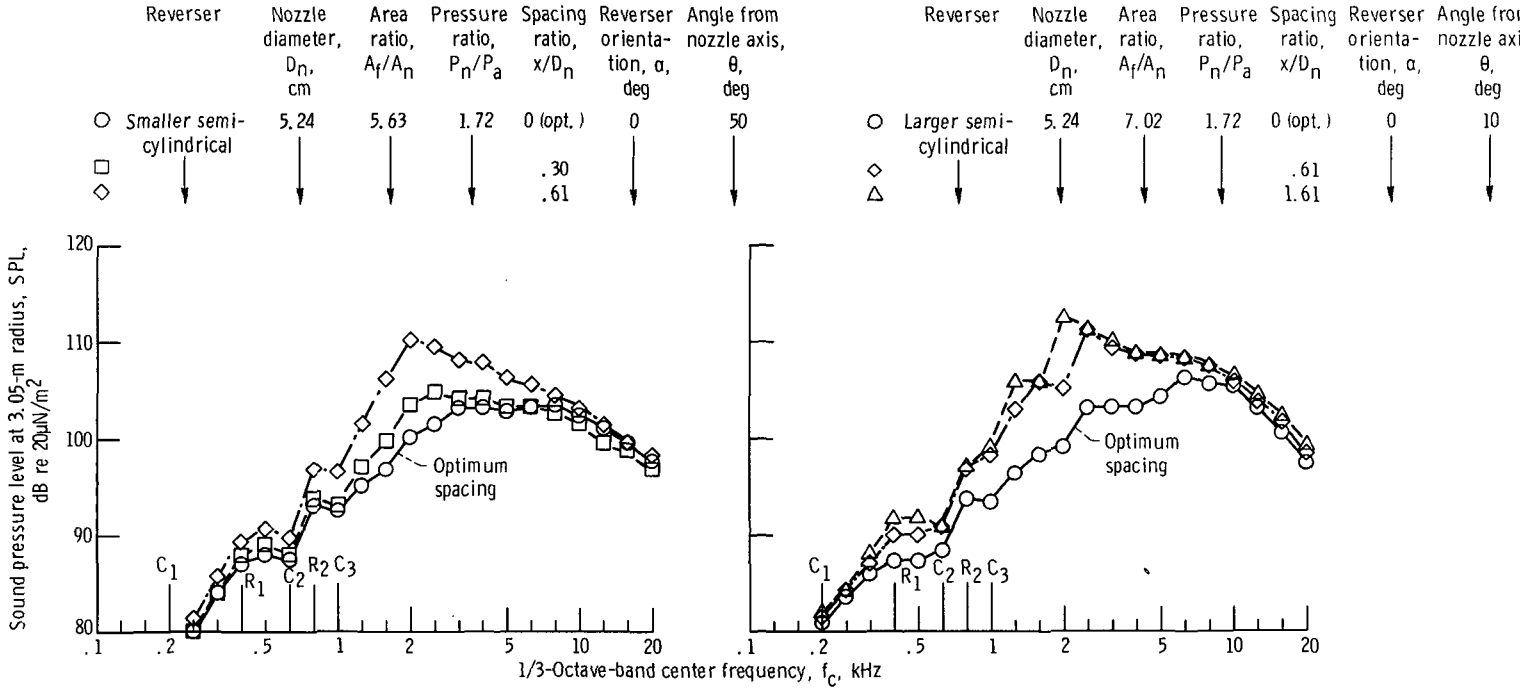

(a) Smaller semicylindrical reverser and 5.24-centimeter-diameter nozzle.

(b) Larger semicylindrical reverser and 5.24-centimeter-diameter nozzle.

Figure 21. - Effect of spacing on sound pressure level spectrum.

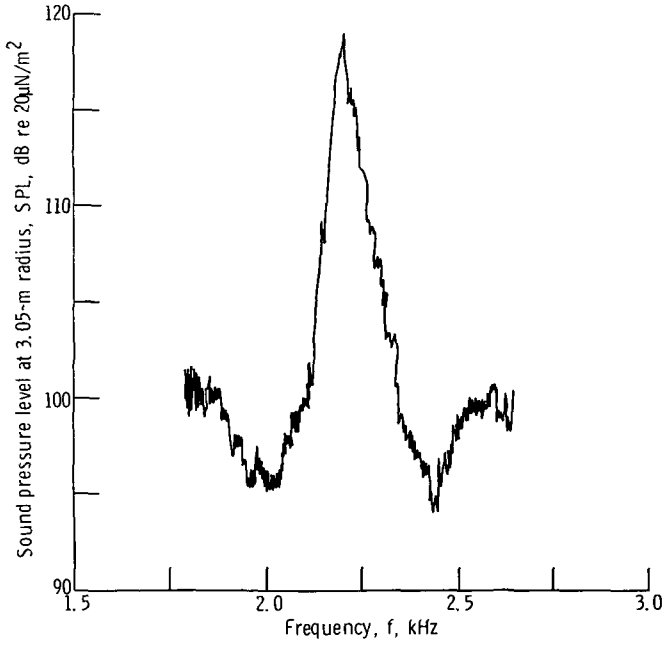

Figure 22. - Partial narrow-band spectrum showing screech obtained with larger cylindrical reverser at spacing ratio x/D_r of 1.61.

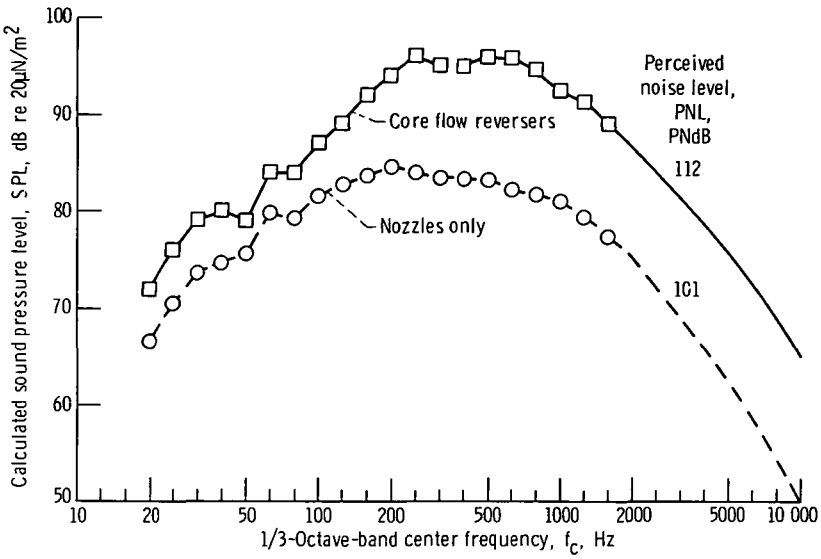

Figure 23. - Calculated sound pressure level spectrum at 152.5-meter (500-ft) sideline for core flow reversers for typical STOL application (based on four 65.5-cm nozzles and cold jets at 295-m/sec nozzle velocity).

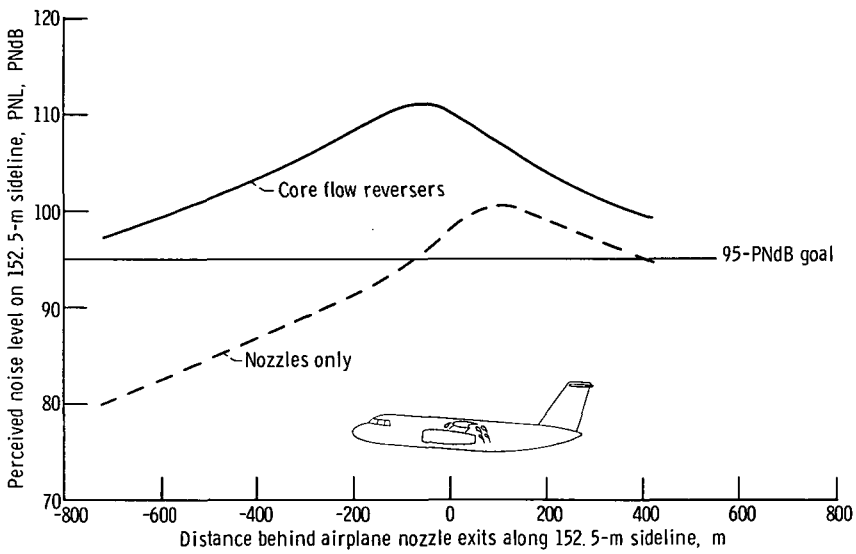

Figure 24. - Perceived noise level along 152.5-meter (500-ft) sideline for core flow reversers for typical STOL application (based on four 65.5-cm nozzles and cold jets at 295-m/sec nozzle velocity).

NATIONAL AERONAUTICS AND SPACE ADMISTRATION
WASHINGTON, D.C. 20546

OFFICIAL BUSINESS
PENALTY FOR PRIVATE USE $300

FIRST CLASS MAIL

POSTAGE AND FEES PAID
NATIONAL AERONAUTICS AND
SPACE ADMINISTRATION

POSTMASTER: If Undeliverable (Section 1
Postal Manual) Do Not Re

"The aeronautical and space activities of the United States shall be conducted so as to contribute . . . to the expansion of human knowledge of phenomena in the atmosphere and space. The Administration shall provide for the widest practicable and appropriate dissemination of information concerning its activities and the results thereof."

—NATIONAL AERONAUTICS AND SPACE ACT OF 1958

NASA SCIENTIFIC AND TECHNICAL PUBLICATIONS

TECHNICAL REPORTS: Scientific and technical information considered important, complete, and a lasting contribution to existing knowledge.

TECHNICAL NOTES: Information less broad in scope but nevertheless of importance as a contribution to existing knowledge.

TECHNICAL MEMORANDUMS: Information receiving limited distribution because of preliminary data, security classification, or other reasons.

CONTRACTOR REPORTS: Scientific and technical information generated under a NASA contract or grant and considered an important contribution to existing knowledge.

TECHNICAL TRANSLATIONS: Information published in a foreign language considered to merit NASA distribution in English.

SPECIAL PUBLICATIONS: Information derived from or of value to NASA activities. Publications include conference proceedings, monographs, data compilations, handbooks, sourcebooks, and special bibliographies.

TECHNOLOGY UTILIZATION PUBLICATIONS: Information on technology used by NASA that may be of particular interest in commercial and other non-aerospace applications. Publications include Tech Briefs, Technology Utilization Reports and Technology Surveys.

Details on the availability of these publications may be obtained from:

SCIENTIFIC AND TECHNICAL INFORMATION OFFICE

NATIONAL AERONAUTICS AND SPACE ADMINISTRATION

Washington, D.C. 20546

Page Intentionally Left Blank